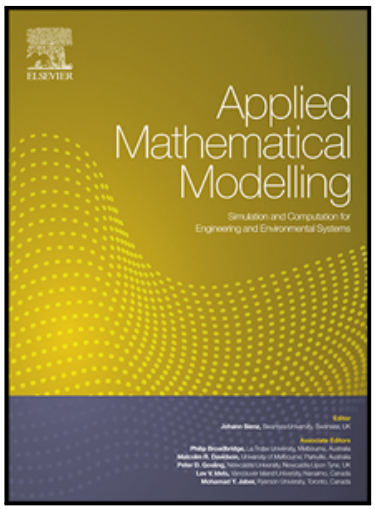

Multi-objective optimization algorithm for analysis of hardened steel turning manufacturing process

Leandro Framil Amorim , Anderson Paulo de Paiva ,
Pedro Paulo Balestrassi , João Roberto Ferreira

PII: S0307-904X(22)00079-8
DOI: https://doi.org/10.1016/j.apm.2022.02.011
Reference: APM 14406

To appear in: *Applied Mathematical Modelling*

Received date: 19 October 2021
Revised date: 11 February 2022
Accepted date: 13 February 2022

Please cite this article as: Leandro Framil Amorim , Anderson Paulo de Paiva , Pedro Paulo Balestrassi , João Roberto Ferreira , Multi-objective optimization algorithm for analysis of hardened steel turning manufacturing process, *Applied Mathematical Modelling* (2022), doi: https://doi.org/10.1016/j.apm.2022.02.011

Highlights:

- Cost and tool life of a hardened steel turning of are properly characterized as typical Poisson random variables.
- Objective functions are simultaneously optimized coupled with their respective variances.
- The proposed method reduces the dimension of the Multi-Objective Optimization problem.
- Proposed Confidence ellipse for Pareto points supports a decision-making based on variability and mean shift.
- A multivariate robust setup for steel turning process is obtained according to the Fuzzy decision-maker.

Multi-objective optimization algorithm for analysis of hardened steel turning manufacturing process

Leandro Framil Amorim [1, *], Anderson Paulo de Paiva [1], Pedro Paulo Balestrassi [1], João Roberto Ferreira [1]

[1] Institute of Industrial Engineering and Management, Federal University of Itajubá, Minas Gerais, Brazil.

* Corresponding author. E-mail address: leandroframorim@gmail.com (L.F. Amorim)

Declarations of interest: None

Abstract: This paper presents a multi-objective optimization algorithm that combines Normal Boundary Intersection method with response surface models of equimax rotated factor scores in order to simultaneously optimize multiples sets of means and variances of manufacturing processes characteristics. The algorithm uses equimax factor rotation to separate means and variances in individual and uncorrelated functions and afterwards combines them in a mean squared error function. These functions are then optimized using Normal Boundary Intersection method generating a Pareto frontier. The optimal solutions found are then filtered according to a 95% non-overlapping confidence ellipses for the predicted values of the responses and posteriorly they are assessed by a Fuzzy decision-maker index established between the volume of each confidence ellipsoid and the Mahalanobis distance between each Pareto point and its individual optima for a given weight. In order to illustrate the practical implementation of this approach, two cases involving the multi-objective optimization of the hardened steel turning process were considered: (a) the AISI 52100 hardened steel turning with CC6050 mixed ceramic inserts and (b) the AISI H13 hardened steel turning with CC 670 mixed ceramic tools. For both cases, the best setup for cutting speed (V), feed rate (f) and depth of cut (d) were adjusted to find the minimal process cost (K_p) and the maximal tool life (T), both responses with minimal variance. The suitable results achieved in these case studies indicate that the proposal may be useful for similar manufacturing processes.

Keywords: Multi-objective Optimization, Normal Boundary Intersection, Factor Analysis, Confidence Ellipse.

Nomenclature

$f_i(\mathbf{x})$	i-th objective function
$g_i(\mathbf{x}) \leq 0$	inequality constraint
$h_i(\mathbf{x}) = 0$	equality constraint
$\mathbf{x}, \mathbf{x}^T = [x_1, x_2, \ldots, x_k]$	solution vector or design vector
$\boldsymbol{\Omega}$	solution space
$\mathbf{x}^T\mathbf{x} \leq \rho^2$	constraint representing the spherical region of a CCD design
ρ	radius of the spherical region
k	CCD design parameters or factors
m, p	number of objective functions or response (output) variables
n	number of experimental runs
r	number of coefficients in the regression models except β_0
$\mathbf{X}_{(n \times r+1)}$	design matrix derived from CCD with n rows and r+1 columns
CCD	Central Composite Design (Rotatable)
$\mathbf{Y}, \mathbf{Y}=[\mathbf{y}_1, \mathbf{y}_2, \ldots, \mathbf{y}_p]$	matrix of response variables
$\boldsymbol{\beta}, \boldsymbol{\beta}^T = [\beta_0, \beta_1, \ldots, \beta_k]$	vector of coefficients of the regression models
$\boldsymbol{\Phi}$	Payoff matrix
$\overline{\boldsymbol{\Phi}}$	scaled (or normalized) form of Payoff matrix
$\mathbf{n}$	Quasi-normal vector
$\overline{\mathbf{F}}(\mathbf{x})$	vector of scaled objective functions
$\overline{f}_i(\mathbf{x})$	Individual scaled objective function
f_i^U	Utopia value for $f_i(\mathbf{x})$
f_i^N	Nadir value for $f_i(\mathbf{x})$
MSE	Mean Square Error
T_i	Target value for $f_i(\mathbf{x})$
$\hat{\sigma}_i^2(\mathbf{x})$	estimated variance equation
MMSE	Multivariate Mean Square Error
$PC_i(\mathbf{x})$	response surface model for the i-th principal component score
ξ_{PCi}	Target for principal component regression model
λ_i, e_i	eigenvalue and eigenvector
Z	Standardized normal variable Z~N(0, 1)
$\mathbf{w}, \mathbf{w}^T = [w_1, w_2, \ldots, w_p]$	vector of weights for multiobjective optimization

$\mathrm{MSE}_i^* = \sigma_{\varepsilon i}^2$	mean square error of the i-th response surface
$\lvert\hat{e}_i\rvert$	predicted standard deviation for the ith response
$R_{e_i}^2$	proportion of explained variance of residuals
Σ, **R**	Variance-covariance and correlation matrices of order *p* x *p*
ℓ_{pm}	Factor loadings (weighted eigenvectors of **Σ** or **R**)
$\mathbf{L} = \left[\sqrt{\lambda_1}e_1, \ldots, \sqrt{\lambda_m}e_m\right]$	Loading vector (*p* x *p*)
$Cov(\boldsymbol{\varepsilon}) = \boldsymbol{\Psi} = \mathrm{diag}(\psi_{11}, \ldots, \psi_{pp})$	Variance-covariance matrix of errors
$\mathbf{z_0}(\mathbf{x_0})$	Positional vector relative to the solution space
	$\mathbf{z_0^T} = \left[\, 1 \;\; x_1 \;\; x_2 \;\; x_3 \;\; x_1^2 \;\; x_2^2 \;\; x_3^2 \;\; x_1x_2 \;\; x_1x_3 \;\; x_2x_3 \right]$
$MSE(FA)_i(\mathbf{x})$	Mean square error function for rotated factor scores
$FA_{\mu_i(T)}(\mathbf{x})$	Response surface model for the rotated factor score of mean
$FA_{\sigma_i^2(T)}(\mathbf{x})$	Response surface model for the rotated factor score of variance
$T_{FA_{\mu_i(T)}}$	Target value for $FA_{\mu_i(T)}(\mathrm{x})$
$MSE(FA)_i^U$	Utopia value for $MSE(FA)_i(\mathbf{x})$
$MSE(FA)_i^N$	Nadir value for $MSE(FA)_i(\mathbf{x})$
s	number of selected fators ($s \leq p$)
$\mathbf{W}_{n\mathbf{x}n}$	diagonal matrix of weights
V	Volume of a confidence ellipse
Γ(.)	Gamma function
S	Sample variance-covariance matrix (*p* x *p*)
MD	Mahalanobis distance
T	Tool life
Kp	Total cost of manufacturing process
V	Cutting Speed (m/min)
f	Feed rate (mm/rev)
d	Depth of cut (mm)
μ^T	Fuzzy decision maker
NBI	Normal Boundary Intersection
OLS	Ordinary Least Squares
MWLS	Multivariate Weighted Least Squares
DOE	Design of Experiments
POE	Propagation of Error

1. Introduction

For a large deal of manufacturing systems, the vital assignment in engineering is to ensure legitimately stable results, as many standardized products as possible. As an initial way to model these systems to be able to control it aiming at the optimal result, researchers have employed design of experiment (DOE) arrays to simultaneously optimize multiple quality characteristics adjusting the process parameters to their best levels. Examples of such approach can be seen in several manufacturing processes like resistance spot welding [1], pulsed gas metal arc welding [2], electro discharge machining [3], hardened steel turning [4-6], free steel machining [7, 8], end milling [9] among others.

On this wise, the quality of products will only be assured if expected values of the performance characteristics are near to their targets, with the least possible dispersion [10]. Eventual mean shifts and an excess of variance are typically occasioned by an inadequate setting of control variables or even by the presence of noise variables [11] and it is particularly observed in mass production lines [12]. In order to increase the product's quality, researchers must minimize, simultaneously, the mean shift and the process variance, discovering the levels of the process control variables that provide an acceptable trade-off between both low variance and a deviation from a previously targeted mean [13]. If there is just one characteristic of interest and if the researcher considers different weights for mean and variance, the problem may be solved by any bi-objective optimization method [12].

Sometimes, it is convenient to use the MSE objective function as a way to agglutinate mean and variance around a specific target for the characteristic of interest [13]. Thusly, it becomes possible to synchronously optimize the process accuracy and precision, concurrently optimizing centrality and dispersion of a process performance variable subject to its respective constraints.

Expanding this reasoning to multi-objective optimization, several works have been carried out considering the simultaneous optimization of several characteristics of processes and their respective variances treating these functions as individual objectives in a goal programming approach [14] or replacing the mean and variance functions directly by MSE indexes [15]. In both cases, the variances are computed from pure replicates [16], residuals from mean models [17], crossed arrays [8] or combined arrays [9]. The aforementioned schemes of computing variance have different costs and precision depending on the number of experiments required, and their use in practice depends on the researcher´s available budget [12].

As a traditional multiobjective optimization method, Normal Boundary Intersection method (NBI) have been also successfully used to solve mean-variance optimization problems in the context of machining process like AISI 12L14 steel turning [8] or AISI 1045 end milling [9]. This method was specifically developed to generate a uniform spread of the Pareto frontier, even in a non-convex solution region [18]. The importance and flexibility inherent to this technique are featured in studies such as [19], in which its strength and suitability were extensively investigated according to the optimization of different and complex types of systems. Pareto frontier is a set of feasible, optimal and nondominated solutions that allows the decision maker to choose the best vector of parameters capable of providing a high level of quality for a specific process of interest [18]. When applied to MSE problems, Pareto frontier presents the feasible solutions found during the trade-off process between mean and variance objective functions. The complexity of problem increases as more objective functions are considered. In this way, for two characteristics there will be four objective functions – being two mean equations and two variance equations; if mean and variance are agglutinate as a MSE index, there will be just two dimensions to the multiobjective problems. Therefore, depending on the scheme adopted to treat the dual mean-variance, larger will be the number of sub-problems involved in the optimization routine [19].

Correlation is also an important aspect to be considered in multiobjective optimization [20] since its negligence may compromises the final results: for example, when two positively correlated objective functions with different sense of optimization are simultaneously optimized the antagonist weights used in a convex combination will change the original correlation signal, creating a set of unrealistic solutions. Besides, since most of multiobjective optimization methods depends on the anchor points to promote normalization or scalarization, their definition based on individual optimization, neglecting the variance-covariance structure of the response data, will originate unrealistic optimization results. The influence of correlation over the optimization results has been faced with several different approaches, as follows: (a) those methods based on the computation and modelling of the correlation of each experiment like as in [21], (b) those considering the variance-covariance matrix of response data to compose a multivariate distance between the vector of expected values and their respective targets [22], (c) those using directly Principal Component Analysis (PCA) to develop latent variables capable of replace the original correlated responses [20] or to create multivariate mean square error indexes [23] and (d), those methods using rotated factor scores (FA) to create uncorrelated objective functions or even relative indexes [24]. It is straightforward that approaches considering the computation of correlation or the covariance

of each designed experiment will require much more replicates than those represented by multivariate techniques and therefore they will be sometimes prohibitive.

Factor Analysis (FA) is a very promising technique capable to treat the correlation influence over optimization schemes [25]. FA is a multivariate statistical technique similar to Principal Component Analysis (PCA) that is capable of form groups of similar variables based on their own correlations. However, while in PCA the latent variables are defined as linear combinations of original variables, in FA the original variables are written as linear combination of factors. The technique is started extracting the eigenvalues and eigenvectors of a variance-covariance or of the correlation matrix and using them as weights to form well-representative scores. These scores are useful to create new uncorrelated objective functions [24] that may be used in any optimization scheme. Since these new dataset keeps a large correlation with the original data, the multivariate objective functions derived from the method will accurately reproduce the behavior of the original system but with uncorrelated functions [26]. Similar to the idea of multivariate mean square error [23], rotated factor scores may also be used to represent means and variance functions in order to compose MSE indexes which, in turn, may be minimized. This approach is capable of improve the mean and minimize the variance of several characteristics simultaneously [26].

The correlation between response variables is also related to the independence of Pareto-optimal solutions. From statistical perspective, a Pareto point is a priori a vector of means that may associated to a variance-covariance matrix when the correlation among the variables is significative. Therefore, when objective functions are correlated, a multivariate confidence region is formed around the optimal solutions. Obviously, these elements will be present in all Pareto-points. Hence, depending on the amount of variability associated to each point, it may occur a considerable number of overlapping confidence ellipses revealing solutions that are not statistically different in true. In this way, all those solutions falling inside the confidence ellipse will be similar or redundant, and will not represent non-dominating alternatives. Otherwise, solutions falling outside the ellipse may will be safely classified as non-dominated ones. In this sense, it is possible to filter the initial Pareto frontier considering the non-overlapping confidence ellipses available.

This filtered set of feasible solutions may will be assessed and classified according to a multi-attribute decision making criteria in order to select the most suitable choice. In this paper, such criteria will be the volume of each confidence ellipsoid – which represents the amount of variability for the original responses in each Pareto-optimal solution - and the Mahalanobis distance between each Pareto point and its individual optima for a given weight. A trade-off between these criteria may be carried out using a Fuzzy decision-maker index [5].

This is the second argument raised in this paper to help the decision maker to choose the best alternatives available.

This work is based on two complementary arguments: (a) the establishment of a MSE index for rotated factor scores and (b) the definition of exclusive Pareto-optimal solutions according to the multivariate uncertainty associated to each Pareto Point. The feasibility and extension of this proposal will be tested with two real hardened steel turning process represented by the simultaneous minimization of cost per manufactured piece (K_p), the maximization of tool life (T) and the minimization of their respective variances: the first case exploring the machining of the AISI 52100 hardened steel [4] and the second one, assessing the machining of AISI H13 hardened steel [27]. In both cases, work pieces with hardness around 55 HRC were machined according to a central composite design for three factors: cutting speed (Vc), feed rate (f) and depth of cut (d).

2. Theoretical background

This section presents the theoretical fundamentals associated with the development of the proposed algorithm and highlights some insights about the integrated use of multiobjective optimization methods, Design of Experiments (DOE) and multivariate statistical analysis.

2.1. Normal boundary intersection

The NBI method was developed to address the deficiencies attributed to the weighted sums method, such as its difficult to generate a uniform spread of Pareto optimal solutions, even when a uniform spread of weight vectors is adopted. If the Pareto set is non-convex, it will imply in a loss of Pareto points on the concave part of the trade-off surface, besides to generate a non-uniformity among the Pareto points along the frontier. Eq. (1) express the original formulation of NBI proposed by [18], as follows:

$$\begin{cases} \underset{(\mathbf{x},t)}{Max} \;\; t \\ S.t.: \;\; \overline{\mathbf{\Phi}}\;\boldsymbol{\beta} + t\hat{\mathbf{n}} = \overline{\mathbf{F}}(\mathbf{x}) \\ \qquad \mathbf{x} \in \boldsymbol{\Omega} \\ \qquad g_j(\mathbf{x}) \le 0 \\ \qquad h_j(\mathbf{x}) = 0 \end{cases} \tag{1}$$

Where $\mathbf{\Phi}$ denotes a p x p payoff matrix shown in Eq. (2), where p is the number of multiple objective functions and $\overline{\mathbf{\Phi}}$ represents its scaled (or normalized) form. $\boldsymbol{\beta}$ is a vector of weights and t is a scalar that is perpendicular to this utopia line. The vector $\mathbf{n}$ is a quasi-

normal vector and $\bar{\mathbf{F}}(\mathbf{x})$ is the vector of scaled objective functions considered in the MOP, **x** denotes the solution vector and **Ω** represents the solution space; $g_j(\mathbf{x})$ and $h_j(\mathbf{x})$ represents respectively the j-th inequality and equality constraint.

$$\mathbf{\Phi} = \begin{bmatrix} f_1^*(x_1^*) & \cdots & f_1(x_i^*) & \cdots & f_1(x_m^*) \\ \vdots & \ddots & & & \vdots \\ f_i(x_1^*) & \cdots & f_i^*(x_i^*) & \cdots & f_i(x_m^*) \\ \vdots & & & \ddots & \vdots \\ f_m(x_i^*) & \cdots & f_m(x_i^*) & \cdots & f_m^*(x_m^*) \end{bmatrix} \tag{2}$$

The elements $f_i(x_i^*)$ are calculated by replacing each individual optimum x_i^* obtained in all objective functions $f_i(x)$, whereas $f_i^*(x_i^*)$ corresponds to x_i^* solution that minimizes the i^{th} objective function. Usually, since objective functions may be represented by different scales or units, they are previously normalized to perform the MOP, producing the scaled version of the pay-off matrix $\bar{\mathbf{\Phi}}$.

The natural choice for the normalization of objective functions uses the Utopia point, $f_i^U(x^*)$, and the Nadir point, $f_i^N(x^*)$, defined as:

$$\bar{f}_i(\mathbf{x}) = \left[\frac{f_i(\mathbf{x}) - f_i^U}{f_i^N - f_i^U} \right], \quad i = 1, 2, \cdots, p \tag{3}$$

NBI could be interpreted as a perpendicular line to the utopia line in a point that is so distant from it. For a generic point (x_0, y_0, z_0), the normal line may be described by $\vec{\mathbf{r}} = [x_0 \quad y_0 \quad z_0]^{\mathbf{T}} + t \times \vec{\nabla} f [x_0 \quad y_0 \quad z_0]^{\mathbf{T}}$ following. Admitting the distance between any point in CHIM and another point on the Pareto frontier is represented by t ($\overline{P_0 P_{\max}}$), so for any point along the CHIM represented by the vector or weights, when t is a maximum, the boundary will be orthogonally intercepted by the normal line.

For bi-objective problems, the NBI formulation becomes:

$$\begin{aligned} &\underset{\mathbf{x}\in\mathbf{\Omega}}{Min} \ \bar{f}_1(\mathbf{x}) \\ &S.t.: \ \bar{f}_1(\mathbf{x}) - \bar{f}_2(\mathbf{x}) + 2\beta_i - 1 = 0 \\ &\quad g_j(\mathbf{x}) \le 0 \\ &\quad 0 \le \beta_i \le 1 \end{aligned} \tag{4}$$

This will be the formulation used in the proposed algorithm.

2.2.MSE objective functions

As proposed by [10] MSE agglutinates the squared distance between the expected value of a response surface, E[f(**x**)] and its target, T, with the variance of f(**x**), Var[f(**x**)]. This convex combination, originally developed without weights, is capable of represent the problem called "Dual response surface" (DRS) and when it is minimized improves the process performance, since finds the optimum **x*** that centers the process inside the tolerance simultaneously reducing its variability. MSE_i may be written for the i-th response of interest as:

$$MSE_i = \left[f_i(\mathbf{x}) - T_i \right]^2 + \hat{\sigma}_i^2(\mathbf{x}) \tag{5}$$

In Eq. (5), **x** represents the vector of process parameters, f(**x**) is an objective function written as a response surface model, $\hat{\sigma}_i^2(\mathbf{x})$ represents the variance equation for the i-th characteristic of interest and T is a target value for f(**x**). Although the expression MSE may assume several other meanings in statistics and engineering, hereinafter this operator will be referred as described in Eq. (5).

2.3. NBI-MMSE Method

Focusing on multiobjective optimization of correlated responses, Bratchell [20] was the first researcher to propose the replacement of original objective functions by response surface models of principal component scores. Using the first principal component, this author showed that is possible to overcome the pitfalls generated by the presence of correlated structures in DOE problems, decomposing them in uncorrelated variables. However, [20] emphasized that PCA is not always enough in problems where the set of multiple responses is not well represented by the first PC-score only. The more responses are considered; the more principal components are required. These components will be linked to subgroups of response variables, however, these latent variables become sparse with low capacity to explain the total variability [4]. This barrier has been partially overcome by [4], considering the response surface of the first principal component as an objective function and the following components as constraints.

In general, the directly use of PCA as a multiobjective optimization strategy has as its main drawback the incapacity to solve problems in which there is a negative relationship between the sense of optimization of PC-scores and the sense of optimization of the original responses. In order to surpass this new obstacle, [23] proposed the concept of "Multivariate

Mean Square Error" (MMSE). In this method, all principal components with eigenvalue larger than the unity are transformed in quadratic distances between the principal component score model and a desirable target and as such, each quadratic distance must be minimized. In this case, the variance was represented by the eigenvalue associated to the respective principal component. This metric was known as $MMSE_i$ and showed to be suitable to treat the problems with divergent optimization directions; however, the index was not capable to overcome the problem of insufficiency of explanation. Therefore, in order to increase the amount of explained variability, a geometric mean of the most representative $MMSE_i$ was suggested as an optimization objective function [23]. MMSE can be established as a multivariate dual response surface, such as:

$$\begin{aligned} &\underset{\mathbf{x}\in\Omega}{Min} \quad MMSE_T = \left[\prod_{i=1}^{k}\left(MMSE_i \middle| \lambda_i \geq 1\right)\right]^{\left(\frac{1}{k}\right)} = \left[\prod_{i=1}^{k}\left[\left(PC_i - \xi_{PC_i}\right)^2 + \lambda_i \middle| \lambda_i \geq 1\right]\right]^{\left(\frac{1}{k}\right)}; k \leq p \\ &St.: \quad g(\mathbf{x}) = \mathbf{x}^{\mathbf{T}}\mathbf{x} \leq \rho^2 \end{aligned} \tag{6}$$

$$\text{Where: } \xi_{PC_i} = \ell_i^T\left[\; Z\left(Y_p \middle| \xi_{Y_p}\right)\right] = \sum_{i=1}^{p}\sum_{j=1}^{q}\ell_{ij}\left[\; Z\left(Y_p \middle| \xi_{Y_p}\right)\right]; i = 1,2,\ldots,p; \quad j = 1,2,\ldots,q$$

Where k is the number of MMSE functions selected according to the significant principal components, PC_i is the fitted second-order polynomial for a principal component score, ξ_{PC_i} is the target value of the i^{th} principal component that must keep a direct relation with the targets established for the original dataset, g(**x**) is the experimental region constraint; ℓ_i represents the eigenvector set associated with the i^{th} principal component, and ξ_{Yp} represents the target associated to the p^{th} original response.

Taking advantage of this idea, Gaudencio et al. [5] proposed to separate the multiple responses of interest in distinct groups defined according to a cluster algorithm, applying PCA to each one of these groups. Retaining only the principal components whose eigenvalues were larger than the unity, a $MMSE_i$ index was associated to each cluster formed. If more than one principal component was required, a geometric operator like described in Eq (6) was adopted. Afterward, each $MMSE_i$ index would be considered as a new objective functions that could be optimized according to the routine and parameters of the NBI method. For bidimensional cases, considering the Utopia and Nadir values of each $MMSE_i$ as $f_i(\mathbf{x}) = MMSE_i(\mathbf{x})$, $f_i^U = MMSE_i^U(\mathbf{x})$ and $f_i^N = MMSE_i^N(\mathbf{x})$, a scalarization is developed, leading to the following optimization system:

$$\begin{aligned} \underset{\mathbf{x}\in\Omega}{Min} \quad & \bar{f}_1(\mathbf{x}) = \left(\frac{MMSE_1(x) - MMSE_1^U(x)}{MMSE_1^N(x) - MMSE_1^U(x)} \right) \\ St.: \quad & \bar{g}_1(\mathbf{x}) = \left(\frac{MMSE_1(x) - MMSE_1^U(x)}{MMSE_1^N(x) - MMSE_1^U(x)} \right) - \left(\frac{MMSE_2(x) - MMSE_2^U(x)}{MMSE_2^N(x) - MMSE_2^U(x)} \right) + 2w - 1 = 0 \\ & \bar{g}_2(\mathbf{x}) = \mathbf{x}^{\mathbf{T}}\mathbf{x} \le \rho^2 \\ & 0 \le w \le 1 \end{aligned} \tag{7}$$

This formulation became known as NBI-MMSE method [5] and represented an evolution in the use of PC-scores as uncorrelated objective functions. When previously using cluster analysis as a manner of decouple the variables of the original data set, [5] in true emulated the concept of "Factor Analysis" that will be described in next sections and, although it seems to be a very similar approach, the method does not have the advantage to "rotate" the data to obtain must suitable groups. Furthermore, through factor analysis, the "grouping" and "rotation" tasks can be performed in a single step, avoiding misleading interpretations. Another advantage in using FA with rotation is possibility to standardize the senses of optimization between an original objective function and a multivariate one. These the main reasons why NBI-RFMSE method is being proposed and tested in this paper.

2.4. Objective function modelling

In this paper, all the objective functions Y_i considered will be estimated using response surface designs and will originate the following generic models:

$$y_i(\mathbf{x}) = \beta_{i0} + \sum_{j=1}^{p} \beta_{ij} x_j + \sum_{j=1}^{p} \beta_{ijj} x_j^2 + \sum_{k=1}^{p} \sum_{l>k}^{p} \beta_{ikl} x_k x_l + \varepsilon_{ikl} \tag{8}$$

The coefficients presented in Eq. (8) are obtained using the Ordinary Least Squares (**OLS**) algorithm, which is based on a design matrix $\mathbf{X}_{(n \text{ x } r+1)}$ for n experimental runs used to estimate the $r+1$ coefficients in a model (including β_0) and on a vector of response $\mathbf{Y}_n$, leading to a vector of coefficients $\boldsymbol{\beta}_{r+1x1}$, such as:

$$\boldsymbol{\beta}_{r+1\times 1} = \left(\mathbf{X}^{\mathbf{T}}_{r+1\times} \mathbf{X}_{n\times r+1} \right)^{-1} \left(\mathbf{X}^{\mathbf{T}}_{r+1\times n} \mathbf{Y}_n \right) \tag{9}$$

OLS is also useful to model variance regression equations. According to Plante [17], when unknown source of variation is present in a process, a considerable part of this information may be hidden in the residuals ε_{ikl} of the mean equation. The variance equation may be found writing a response surface model for absolute value of the residuals ε_{ikl} of the

mean model. Therefore, the variance equation of the i^{th} performance characteristic may be expressed as:

$$Var\left[\hat{y}(x)\right] = \sigma_i^2(x) \cong \left|\hat{e}_i\right|^2 + \left(1 - R_{e_i}^2\right)\mathrm{MSE}_i^* \tag{10}$$

Where: $\mathrm{MSE}_i^* = \sigma_{\varepsilon i}^2$ is the mean square error resulting from the response surface estimated for the i^{th} performance characteristic in Eq. (8); $\left|\hat{e}_i\right|$ is equal to predicted standard deviation for the i^{th} performance characteristic, computed using the absolute values of the residuals of mean. Such models present a proportion of explained variance given by $R_{e_i}^2$.

2.5. Factor Analysis

Factor Analysis (FA) is a multivariate statistical technique capable of form groups of variables based on their correlations [25]. In this statistical procedure, the difference between the random dependent variables (x_p) and their respective mean (μ_p) is expressed as a linear combination of common factors F_m (unobserved random latent variables), their respective coefficients ℓ_{pm} (called loadings) and specific factor ε_p (called error).

The factors F_m are centered, uncorrelated and standardized, also $\mathbf{F}$ and $\boldsymbol{\varepsilon}$ are independent, with null expected value and unitary variance. Besides, the covariance between any two factors F_m and F_k, $_{m \neq k}$, are null. This implies that factors are also uncorrelated variables. It is also assumed that $E(\varepsilon_p) = 0$, $Var(\varepsilon_p) = \psi_p$, $Cov(\varepsilon_p, \varepsilon_k) = 0$, $p \neq k$, $Cov(\varepsilon_p, F_m) = 0$ for all p and m. Since $Cov(\boldsymbol{\varepsilon}) = \boldsymbol{\Psi} = \mathrm{diag}(\psi_{11}, \ldots, \psi_{pp})$, it is straightforward that covariance structure for the orthogonal factor model may be written as $\boldsymbol{\Sigma} = Cov(\mathbf{x}) = \mathbf{L}\mathbf{L}' + \boldsymbol{\Psi}$, with $Cov(\mathbf{x}, \mathbf{F}) = \mathbf{L}$ like demonstrated in [25].

The specific purpose of FA is therefore to identify the loadings (or coefficients) that allows to write each variable x_p as a linear combination of factors F_m, with possible errors represented in $\boldsymbol{\Psi}$. Frequently, a clear interpretation of the extracted factors can be improved by rotating them, which promotes the most disjoint groups possible, each being associated to one specific factor [25]. Among the main orthogonal rotation methods are Quartimax, Orthomax, Varimax and Equimax [25].

Factor Analysis (FA) allows the storage of the most of information contained in the original variables of a group into a new latent variable called "Factor Score". This new variable may be found using the transformation $\mathrm{F}_a = \left[Z\left(Y_p\right)\right]\left[\mathbf{L}(\mathbf{L}^{\mathbf{T}}\mathbf{L})^{-1}\right]$, where the loading vector is equals to $\mathbf{L} = \left[\sqrt{\lambda_1}e_1, \ldots, \sqrt{\lambda_m}e_m\right]$, with e_i and λ_i representing the eigenvectors and

eigenvalues of the variance-covariance (**Σ**) or correlation (**R**) matrices of y_p with Z(y_p) being its standardized value [23].

In this paper, factor scores will be used to replace the original responses variables Y_p creating a new set of independent objective functions. Depending on the correlation structure, it is also possible to reduce the dimension of data, since one factor may adequately represent more than one original variable. Such compression depends on the results observed during the eigenanalysis.

2.6. Confidence ellipses for predicted values

As shown in [25], the vector of expected values of multivariate regression models $f_i(\mathbf{x})$ at the point $\mathbf{x_0}$ is given by $\boldsymbol{\beta}^{\mathbf{T}}\mathbf{z_0}$ ($\mathbf{x_0}$), where **β** is the matrix of coefficients of the regression models involved; $\mathbf{z_0}$ is a positional vector established according to the elements of the assumed regression models $f_i(\mathbf{x})$. Therefore, the 100(1-α) % confidence ellipsoid for the mean vector at a given point $\mathbf{x_0}$ may be written as:

$$\left[\boldsymbol{\beta}^{\mathbf{T}}\mathbf{z}(\mathbf{x_0})-\hat{\boldsymbol{\beta}}^{\mathbf{T}}\mathbf{z}(\mathbf{x_0})\right]^{\mathbf{T}}\left(\frac{n}{n-r-1}\hat{\boldsymbol{\Sigma}}\right)^{-1}\left[\boldsymbol{\beta}^{\mathbf{T}}\mathbf{z}(\mathbf{x_0})-\hat{\boldsymbol{\beta}}^{\mathbf{T}}\mathbf{z}(\mathbf{x_0})\right]\leq \mathbf{z}^{\mathbf{T}}(\mathbf{x_0})\left(\mathbf{X}^{\mathbf{T}}\mathbf{X}\right)^{-1}\mathbf{z}(\mathbf{x_0})\left[\frac{m(n-r-1)}{n-r-m}F_{m,n-r-m}(\alpha)\right] \quad (11)$$

In Eq. (11), $\mathbf{X}_{(n \times r+1)}$ represents the design matrix of multivariate regression models, *m* is the number of responses, *n* is the number of observations and *r* is equal to the number of coefficients except β_0. $\hat{\Sigma}$ is the variance-covariance matrix of the residuals of the adjusted models, and $F_{m,n-r-m}(\alpha)$ is the upper (100α)-th percentile of an F-distribution with *m* and *n-r-m* degrees of freedom. It is also worth noting that each ellipse is inclined according to an angle θ which represents the correlation observed in the data set [25].

In order to drawn a 100(1-α) % confidence ellipse it is suggested the following expression:

$$\mathbf{z}_0^{\mathbf{T}}\hat{\boldsymbol{\beta}}_i+\sqrt{\frac{m_{ii}}{n-r-m}F_{m,n-r-m}(\alpha)\ \left[\mathbf{z}^{\mathbf{T}}(\mathbf{x_0})\left(\mathbf{X}^{\mathbf{T}}\mathbf{X}\right)^{-1}\mathbf{z}(\mathbf{x_0})\right]}\times\begin{bmatrix}\sqrt{\lambda_1} & 0\\ 0 & \sqrt{\lambda_2}\end{bmatrix}\times\begin{bmatrix}e_{11} & e_{12}\\ e_{12} & e_{22}\end{bmatrix}\times\begin{bmatrix}\cos\phi\\ \sin\phi\end{bmatrix} \quad (12)$$

The eigenvalues (λ_1, λ_2) and eigenvectors (e_{11}, e_{12}, e_{21}, e_{22}) used are extracted from the variance-covariance matrix of the residuals of the adjusted models ($\mathbf{n}\hat{\boldsymbol{\Sigma}}$) and the ellipse is parameterized according to the range $0 \leq \phi \leq 2\pi$.

The models adequacy may be improved using a multivariate least squares algorithm (MWLS) like as described in Eq. (13), with a diagonal matrix of weights ($\mathbf{W}_{nxn}$) defined as the inverse of squared Mahalanobis Distance (MD) established for the residuals of first OLS models, like shown by Eq. (14).

$$\hat{\boldsymbol{\beta}}_{MWLS_{(r+1\times1)}} = \left(\mathbf{X}^{\mathbf{T}}_{r\times n}\mathbf{W}_{n\times n}\mathbf{X}_{n\times r}\right)^{-1}\left(\mathbf{X}^{\mathbf{T}}_{r\times n}\mathbf{W}_{n\times n}\mathbf{Y}_{n}\right) \tag{13}$$

$$MD = \sqrt{\mathbf{e}^{\mathbf{T}}_{1\times p}\left(n\hat{\boldsymbol{\Sigma}}_{p\times p}\right)^{-1}\mathbf{e}_{p\times 1}} \tag{14}$$

Where: MD represents in this case the Mahalanobis distance of the residuals; $\mathbf{e}_{px1}$ represents the vector of the residuals for the p OLS models in the n-th run; $\hat{\boldsymbol{\Sigma}}_{p\times p}$ denotes the variance-covariance matrix of the residuals of the p response surface models.

The confidence ellipsoid for each predicted Pareto point will be properly found replacing Eq. (13) into Eq. (12), like will be detailed the following propositions.

3. Development of proposed method

The multi-objective optimization algorithm developed for the analysis of hardened steel turning manufacturing process (NBI-RFMSE) is created according to some assumptions described in the theoretical background of **Section 2** and they are detailed in the following propositions.

3.1. Proposition 1 – MSE of rotated factors scores

Suppose there are p correlated responses of interest from which may be derived a pair of mean and variance objective functions, both written in terms of a vector of control variables (x). Also consider that Factor Analysis (FA) may be applied to generate independent objective functions in terms of rotated factor scores. If means and variances may be replaced by response surface models of these scores and if they are posteriorly agglutinated into a MSE function [26], then it is possible to write that:

$$MSE(FA)_i(\mathbf{x}) = \left[FA_{\mu_i(T)}(\mathbf{x}) - T_{FA_{\mu_i(T)}}\right]^2 + \left[FA_{\sigma_i^2(T)}(\mathbf{x})\right] \tag{15}$$

$$T_{\mathrm{FA}_{(\mu)i}} = e_i^T\sqrt{\lambda_i}\left[Z\left(Y_p \mid T_{Y_p}\right)\right] = \sum_{i=1}^{p}\sum_{j=1}^{q} e_{ij}\sqrt{\lambda_{ij}}\left[Z\left(Y_p \mid T_{Y_p}\right)\right] \tag{16}$$

In Eq. (15), $MSE(FA)_i$ represents the "means square error" of the i-th rotated factor score surface model, $FA_i(\mathbf{x})$. Eq. (16) shows how the target for the rotated factor score models, T_{FAi}, can be obtained from the targets of the original variables.

3.2. Proposition 2 – Targets obtained by individual optimization

The target values for the original objective functions, T_{Y_p}, may be obtained by individual optimization or may be settled up according to decision maker´s preference as also the targets for the rotated factor scores equations, $T_{\mathrm{FA}_{(\mu)1}}$ and $T_{\mathrm{FA}_{(\mu)2}}$. It is only need to observe the sense of optimization that allows the compatibility between responses and factor scores models. For a minimization case, the value of T_{FAi} may be defined as:

$$T_{FA_i} = \begin{cases} \underset{\mathbf{x}\in\Omega}{Min} \;\; FA_i(\mathbf{x}) \\ S.t.: \;\; g(\mathbf{x}) = \mathbf{x}^{\mathbf{T}}\mathbf{x} - \rho^2 \le 0 \end{cases} \tag{17}$$

Where $\rho = 2^{k/4}$ represents the radius of the spherical region of a CCD design for *k* input factors [4].

3.3. Proposition 3 – Utopia and Nadir points defined as optimization of MSE(FA)i

The individual optimization of Eq. (15) allows the definition of the Utopia and Nadir points that may be written as:

$$\begin{aligned} Utopia: \;\; MSE(FA)_i^U &= \begin{cases} \underset{\mathbf{x}\in\Omega}{Min} \;\; MSE(FA)_i(\mathbf{x}) = \left[FA_i(\mathbf{x}) - T_{FA_i}\right]^2 + \sigma^2(FA_i) \\ S.t.: \;\; g(\mathbf{x}) = \mathbf{x}^{\mathbf{T}}\mathbf{x} - \rho^2 \le 0 \end{cases} \\ Nadir: \;\; MSE(FA)_i^N &= \begin{cases} \underset{\mathbf{x}\in\Omega}{Max} \;\; MSE(FA)_i(\mathbf{x}) = \left[FA_i(\mathbf{x}) - T_{FA_i}\right]^2 + \sigma^2(FA_i) \\ S.t.: \;\; g(\mathbf{x}) = \mathbf{x}^{\mathbf{T}}\mathbf{x} - \rho^2 \le 0 \end{cases} \end{aligned} \tag{18}$$

With these results, it is possible to normalize the $MSE(FA)_i$ functions for bi-objective optimization problems, such as:

$$\bar{f}_i = \frac{MSE(FA)_i(\mathbf{x}) - MSE(FA)_i^U}{MSE(FA)_i^N - MSE(FA)_i^U} \quad i = 1,\ 2, \cdots, s; \quad s \le p \tag{19}$$

3.4. Proposition 4 – NBI-RFMSE method

If the former propositions are attended, it is possible to write the formulation of NBI-RFMSE method as:

$$\begin{aligned} &\underset{\mathbf{x}\in\boldsymbol{\Omega}}{Min}\ \ \bar{f}_1 = \left[\frac{MSE(FA)_1(\mathbf{x}) - MSE(FA)_1^U}{MSE(FA)_1^N - MSE(FA)_1^U}\right] \\ &S.t.: \left[\frac{MSE(FA)_1(\mathbf{x}) - MSE(FA)_1^U}{MSE(FA)_1^N - MSE(FA)_1^U}\right] - \left[\frac{MSE(FA)_2(\mathbf{x}) - MSE(FA)_2^U}{MSE(FA)_2^N - MSE(FA)_2^U}\right] + 2\beta_i - 1 = 0 \\ &\quad g(\mathbf{x}) = \mathbf{x}^{\mathbf{T}}\mathbf{x} - \rho^2 \le 0 \\ &\quad 0 \le \beta_i \le 1 \end{aligned} \tag{20}$$

The Pareto frontier is then obtained running Eq. (20) iteratively for different weights. Since the objective functions involved are response surface models, the several optimal and feasible solutions will just be a vector of expected values for the Pareto-optimal and each solution will be associated to a multivariate confidence region.

3.5. Proposition 5 - Confidence ellipses for Pareto points

Suppose the existence of a confidence ellipsoid for each solution in a given Pareto frontier, considering the vector of expected mean values as its centroid and a variance-covariance matrix written in terms of the estimated variance functions. This ellipsoid may be defined as:

$$\mathbf{z}_0^{\mathbf{T}}\hat{\boldsymbol{\beta}}_{\mathrm{MWLS}\,i} + \sqrt{\frac{m_{ii}}{n-r-m}F_{m,n-r-m}(\alpha)\left[\mathbf{z}^{\mathbf{T}}(\mathbf{x}_0)\left(\mathbf{X}^{\mathbf{T}}\mathbf{W}\mathbf{X}\right)^{-1}\mathbf{z}(\mathbf{x}_0)\right]} \times \begin{bmatrix}\sqrt{\lambda_1} & 0\\ 0 & \sqrt{\lambda_2}\end{bmatrix} \times \begin{bmatrix}e_{11} & e_{12}\\ e_{12} & e_{22}\end{bmatrix} \times \begin{bmatrix}\cos\phi\\ \sin\phi\end{bmatrix} \tag{21}$$

Where $\hat{\boldsymbol{\beta}}_{MWLS_i}$ follows Eq. (13), $\mathbf{W}_{n\mathbf{x}n}$ is a diagonal matrix of weights whose elements are defined as the inverse of squared Mahalanobis Distance (MD) established for the residuals of first OLS models, Eq. (14), and $\mathbf{z}_0^{\mathbf{T}} = \left[\,1\ \ x_1\ \ x_2\ \ x_3\ \ x_1^2\ \ x_2^2\ \ x_3^2\ \ x_1x_2\ \ x_1x_3\ \ x_2x_3\,\right]$ for a full quadratic model with k=3 factors.

The confidence ellipsoid is just a pictorial representation of multivariate hypothesis test for a vector of means. When two vectors of means are statistically equal, then there will

be an overlapping of their confidence ellipses. In this way, non-overlapping confidence ellipses will suggest the existence of statistically different Pareto points.

3.4. Proposition 4 – Fuzzy Decision-Maker: Volume of Confidence Ellipse versus Mahalanobis Distance

Both mean shift and variance are important during the optimization, however, depending on the weights imposed for a given Pareto solution, precision and accuracy will present different values along the frontier. Therefore, to choose the most appropriate solution according to the decision maker´s preference, it is necessary to evaluate the degree of importance of the elements used to discriminate Pareto solutions, i.e., the Mahalanobis distance (MD) and the ellipse volume (V). Adapting Mahalanobis Distance (MD) to measure the process mean vector "shift" it is possible to write:

$$\begin{aligned} \mathrm{MD} = \mathrm{D}_i &= \sqrt{\left(\mathrm{E}(\mathbf{x}_0) - \mathrm{target}\right)^{\mathbf{T}} \left(\mathbf{S}\right)^{-1} \left(\mathrm{E}(\mathbf{x}_0) - \mathrm{target}\right)} \\ &= \left(\begin{bmatrix} E\left[f_1(x_0)\right] - E\left[f_1(x_0^*)\right] \\ E\left[f_2(x_0)\right] - E\left[f_2(x_0^*)\right] \end{bmatrix}^T \begin{bmatrix} \mathrm{var}\left[f_1(x_0)\right] & \gamma \\ \gamma & \mathrm{var}\left[f_2(x_0)\right] \end{bmatrix}^{-1} \begin{bmatrix} E\left[f_1(x_0)\right] - E\left[f_1(x_0^*)\right] \\ E\left[f_2(x_0)\right] - E\left[f_2(x_0^*)\right] \end{bmatrix} \right)^{\frac{1}{2}} \end{aligned} \quad (22)$$

In Eq. (22), the parameter γ represents the covariance between $f_1(\mathbf{x})$ and $f_2(\mathbf{x})$, with ($\mathbf{S}_{pxp}$) representing their variance-covariance matrix.

The amount of variability associated to each optimal mean vector of Pareto frontier may be evaluated using the volume of 100(1-α) % confidence ellipse associated to this mean vector. Like as presented in [25], the ellipse volume can be expressed as:

$$V = \frac{(2\pi)^{\frac{p}{2}}}{p} \Gamma\left(\frac{p}{2}\right) \times |\mathbf{S}|^{1/2} \times \left\{ \sqrt{\frac{p(n-1)}{n(n-p)} F_{(p,n-p)}(\alpha)} \right\}^p \quad (23)$$

Where: $\Gamma(x) = \int_0^\infty u^{x-1} e^{-u} du$.

In Eq. (23), the parameter *p* represents the number of dimensions (or variables) considered in the problem, *n* is the number of degrees of freedom of the error term, α is the significance level and Γ(.) represents the gamma function [25].

The discrimination between MD and V may be established using the concept of Fuzzy decision maker [28, 29], in which membership functions are built for the attributes according to the arbitrary degree of preference manifested by the decisor. To execute this step, it is necessary to parameterize Utopia and Nadir values for each function, calculating the memberships and ranking them according to Fuzzy logic scenario, in the range [0, 1].

In this context, it is desirable that functions have the smallest Mahalanobis distance, as well as the smallest confidence ellipse volume. The membership functions are expressed according to Eq. (24):

$$\mu_{\mathrm{D}i}=\begin{cases}1, & \mathrm{D}_i \le \mathrm{D}_i^{\mathrm{U}} \\ \dfrac{\mathrm{D}_i^{\mathrm{N}}-\mathrm{D}_i}{\mathrm{D}_i^{\mathrm{N}}-\mathrm{D}_i^{\mathrm{U}}} & \mathrm{D}_i^{\mathrm{U}}<\mathrm{D}_i<\mathrm{D}_i^{\mathrm{U}} \\ 0, & \mathrm{D}_i \ge \mathrm{D}_i^{\mathrm{N}}\end{cases} \quad , \quad \mu_{\mathrm{V}i}=\begin{cases}1, & \mathrm{V}_i \le \mathrm{V}_i^{\mathrm{U}} \\ \dfrac{\mathrm{V}_i^{\mathrm{N}}-\mathrm{V}_i}{\mathrm{V}_i^{\mathrm{N}}-\mathrm{V}_i^{\mathrm{U}}} & \mathrm{V}_i^{\mathrm{U}}<\mathrm{V}_i<\mathrm{V}_i^{\mathrm{U}} \\ 0, & \mathrm{V}_i \ge \mathrm{V}_i^{\mathrm{N}}\end{cases} \tag{24}$$

Fuzzy decision maker (μ^T) is defined as the weighted sum of membership functions considered [5], assuming the form of Eq. (25), such as:

$$\mu^{\mathrm{T}}=\sum_{n=1}^{k}\left(w_i\mu_{\mathrm{V}i}+\left(1-w_i\right)\mu_{\mathrm{D}i}\right)=0.15\mu_{\mathrm{V}i}+0.85\mu_{\mathrm{D}i} \tag{25}$$

Then, the better Pareto solution will be that with the highest Fuzzy decision maker (μ^T) value. It is worth mentioning that in this paper, displacement of means will be consider more important than variances, with an arbitrated ratio about 85/15.

4. Material and methods

The propositions presented in the **Section 3** allows the establishment of generic framework to address multiobjective optimization problems involving multiple dual response surfaces. Starting with an experimental design for multiples responses – a CCD in this case -, the models for the original responses must be estimated and their respective residuals, stored. Afterwards, squared residuals are taken to create the variance data. According to the literature [30], the presence of unknown "noise" variables or the selection of non-normal distributed responses (mainly Poisson or Binomial models) will generally be detected and quantified by the residuals of mean models. Hence, using Eq. (9) and (10), the mean and variance models of each response of interest are obtained. This is basically the **Step 1** of the proposed framework.

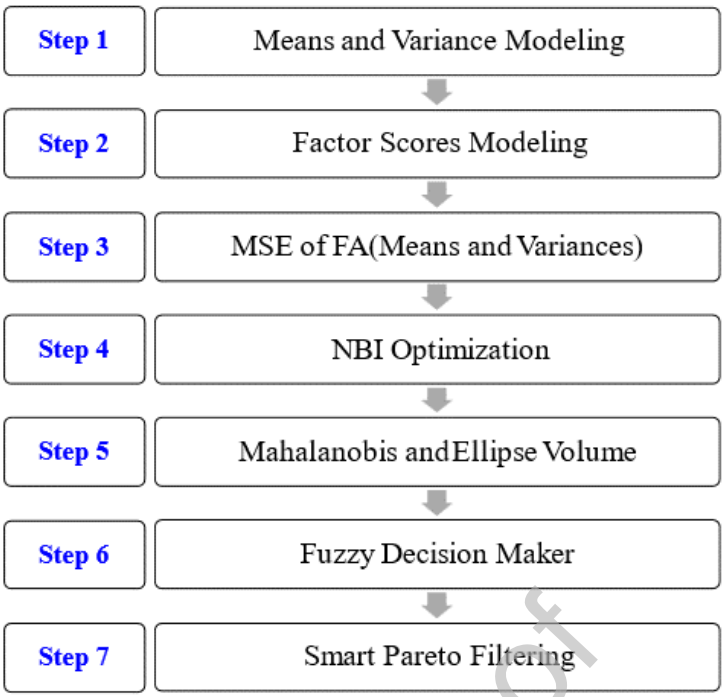

Fig. 1 – Multiobjective robust optimization framework.

After correlation analysis of the data, both mean and variance data are transformed into equimax rotated factor scores to originate the non-correlated models. Although, any rotation method could be employed in this case, "Equimax" will promote factor with similar associated eigenvalues. This task characterizes the **Step 2**. Further, the dimensionality of optimization problem is reduced by agglutinating F_a objective functions into MSE-FA functions (**Step 3**). Then, these functions are simultaneously optimized applying the NBI method, resulting in a complete Pareto frontier (**Step 4**). In sequence, a confidence ellipse is established for each point of Pareto frontier according to the respective mean vector and variance-covariance matrix obtained during the optimization. Finally, for each solution considered, volumes of confidence ellipses are calculated, as well as Mahalanobis Distance between mean and the respective target (**Step 5**). So, these two measures compound a Fuzzy decision maker (**Step 6**) which, in turns, allows the choice of the most appropriate parameters for the process, according to the declared researcher´s interest. Applying the concept of non-overlapping confidence regions, the most suitable Pareto-optimal solution is found (**Step 7**). The **Fig. 1** presents an overview of this sequence, named as NBI-RFMSE method.

The seven steps suggested in **Fig. 1** are following detailed.

Step 1 - Modeling of Mean and Variance: Starting with DOE, it is generated a central composite response surface design considering process variables (factors) and their respective levels. After running the experimental design, the matrix of responses is obtained. Pearson

correlation analysis is performed to investigate the existence of dependence among the responses (experimental data). Subsequently, the regression models are obtained according]ng to OLS method.

Next, for each response of interest, the residuals of OLS models are stored. It is worth standing to emphasize that anomalous behavior on the residuals may be detected using graphical approaches and can indicate the presence of non-normal response variables. Processing these residuals with POE or Poisson regression the variance equations may be found. Besides the expected correlation among the original responses, heteroscedastic models will generally present a significative correlation between expected values and variances. Therefore, PCFA approach may be used to decouple the response variables into an uncorrelated dataset.

Step 2 – Modeling of Factor Scores: FA is performed to propitiate independent functions and then to avoid correlated variables in the subsequent optimization. In the FA it is possible that data could be separated independently that is, effectively representing mean and variance for each process response. The Factor score of each response is modeled by OLS with the same RSM design.

Step 3 - Agglutination of FA of Mean and Variance into a MSE metric: The pairs of factor scores of mean and variance models for each process response are agglutinated into a single MSE objective function. Such approach reduces a four-dimensional problem (four FA models) to a two-dimensional one.

Step 4 - NBI Optimization: Start obtaining the individual optima for each MSE-FA function using the experimental region as constraint. Generalized Reduced Gradient (GRG) algorithm may be applied in this task. Then, after writing the payoff matrix, promote the scaling of MSE-FA functions; perform Normal Boundary Intersection method with MSE-FA functions obtained in the **Step 3** according to Eq. (20).

Step 5 – Calculation of Mahalanobis Distance, Confidence Ellipse and Volume: For each Pareto point, the variance-covariance matrix (**S**) is defined considering the variances estimated. The covariance may be estimated using the correlations observed among the original responses and the variances previously obtained, such as $\gamma = \rho_{ij}\sqrt{\sigma^2\left[f_i(\mathbf{x})\right]\times\sigma^2\left[f_j(\mathbf{x})\right]}$, $i \neq j$. In the sequence, find the values of Mahalanobis distance [Eq. (27)] and ellipse volume [Eq. (28)] for each Pareto solution. In the calculation, considers *p* equals to the number of original responses and *n* as the degree of freedom of error term observed in the ANOVA test for regression models.

Step 6 – Calculation of Fuzzy Decision Maker: The solutions must be evaluated according two perspectives: accuracy and precision. Establish the Fuzzy decision maker (μ^T) like as defined in Eq.(31) , considering two membership functions: Mahalanobis distance (μ_{Di}) and confidence ellipse volume (μ_{Vi}) as Eq. (25). Choose weights for these two memberships according to some prior preference. Ultimately, the highest Fuzzy indicator will point out the best Pareto frontier solution according to the precision and accuracy perspectives.

Step 7 – Smart Pareto Filtering: Draw ellipses according to Eq. (21) for all Pareto points and exclude those solutions whose confidence regions are overlapped.

5. Numerical examples and results

The proposed algorithm will be illustrated using two numerical examples derived from real and experimental data of manufacturing processes: (a) a follow-along case based on the data of hardened steel turning of AISI 52100 with CC6050 mixed ceramic [4] and a short case using the same manufacturing process but for a different work piece material (AISI H13 hardened steel) and a different machining tool (CC 670 mixed ceramic insert) [27].

5.1. Multiobjective optimization of AISI 52100 hardened steel turning: a follow-along case.

This item presents the multiobjective optimization of the AISI 52100 steel turning process proposed in [4]. This experiment used cylindrical work pieces in dimensions of ϕ49 x 50mm; all of them were quenched and tempered to achieve a hardness between 53 and 55 HRC, up to a depth of 3 mm below the tool surface. The machine tool used was a CNC lathe with power of 5,5 KW in the spindle motor, with conventional roller bearings. The mixed ceramic (Al_2O_3 + TiC) inserts used were coated with a very thin layer of titanium nitride (TiN) presenting a chamfer on the edges. Their ISO code was CNGA 120408 S01525 and they were made by Sandvik Coromant (Sandvik class CC6050). The tool holder (ISO code DCLNL 1616H12) presented negative geometry with entering angle of κ_r = 95°. Tool flank wear measurements (VB_{max}) were taken through an optical microscope and the tool breaking point was used as criteria for the end´s life.

Under such conditions, a central composite design was defined according to the range of setups described in **Table 1**, resulting in a CCD with 18 runs like shown in **Table 2**.

Table 1 – CCD factors levels

Parameter	Symbol	Unit	Levels (coded)				
			−1.633	−1	0	1	1.633
Cutting speed	*V*	m/min	187.34	200	220	240	252.66
Feed rate	*f*	mm/rev	0.0342	0.05	0.075	0.1	0.1158
Depth of cut	*d*	mm	0.1025	0.15	0.225	0.3	0.3475

In the original work [4], seven responses were considered: surface roughness, tool life, tool wear, cutting time, process costs and material removal rate.

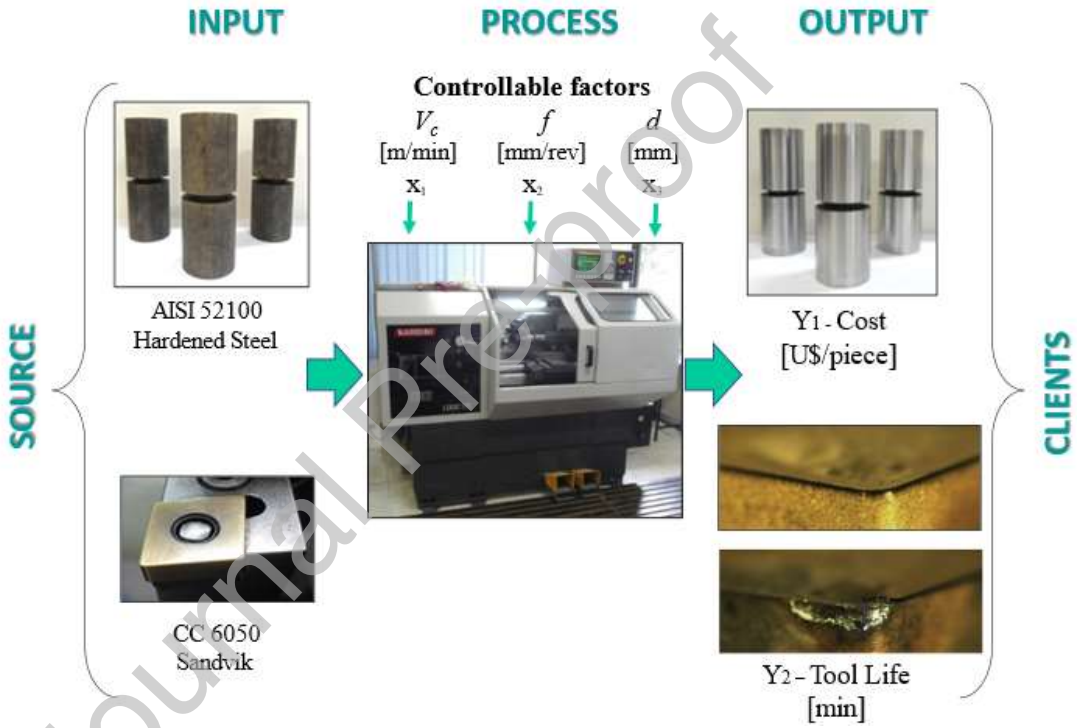

Fig. 2 - SIPOC of AISI 52100 hardened steel turning.

The SIPOC (Source-Input-Process-Output-Client) of **Fig. 2** summarizes the main characteristics of AISI 52100 hardened steel turning. For sake of illustration, a simpler bi-objective problem involving only the Tool life (T) and process costs (Kp) was chosen.

Starting with **Step 1**, it is defined a CCD for the parameters defined in **Table 1**. The characteristics of the CCD described in **Table 2** are: 3 input factors, 1 replicate, 18 runs, 2 blocks. Also, for full two-level factorial, 8 cube points, 2 center points in cube, 6 axial points, 2 center points in axial and the distance of each axial point $\alpha = 1.633$.

Table 2 – Cutting parameters and responses for the CCD

Runs	Block	*V*	*f*	*d*	T	K_p	σ^2(T)	σ^2(Kp)
1	1	200.00	0.0500	0.1500	16.75	7.70	1.000	1.059
2	1	240.00	0.0500	0.1500	11.50	6.41	3.199	1.029
3	1	200.00	0.1000	0.1500	9.85	3.85	1.531	1.198
4	1	240.00	0.1000	0.1500	8.50	3.21	1.228	1.045
5	1	200.00	0.0500	0.3000	11.50	3.85	1.228	1.038
6	1	240.00	0.0500	0.3000	7.45	3.21	1.525	1.119
7	1	200.00	0.1000	0.3000	8.20	1.92	3.214	1.025
8	1	240.00	0.1000	0.3000	6.25	1.60	1.000	1.037
9	1	220.00	0.0750	0.2250	8.60	3.11	2.344	1.672
10	1	220.00	0.0750	0.2250	6.80	3.10	2.344	1.672
11	2	187.34	0.0750	0.2250	10.10	3.65	1.880	1.063
12	2	252.66	0.0750	0.2250	7.60	2.71	1.873	1.049
13	2	220.00	0.0342	0.2250	17.50	6.82	5.783	1.033
14	2	220.00	0.1158	0.2250	7.20	2.01	5.833	1.034
15	2	220.00	0.0750	0.1025	12.00	6.82	1.001	1.238
16	2	220.00	0.0750	0.3475	6.70	2.01	1.001	1.138
17	2	220.00	0.0750	0.2250	7.20	3.09	2.344	1.672
18	2	220.00	0.0750	0.2250	9.10	3.11	2.344	1.672

Source: Adapted from Paiva et al. [4] – coauthor.

In sequence, the correlation between the T and Kp is investigated. Proceeding with the Pearson´s correlation analysis, it is observed a positive and significative correlation between *T* and K_p around 0.776, with P-value equal 0.000. These responses are positively correlated and their sense of optimization is opposite; while is expected that tool life (T) must be maximized, process costs (Kp) must be minimized. In other words, these responses represent a natural case of conflict between the objectives, with different anchor points.

Table 3 presents the full quadratic models for means, variances and rotated factor scores, with high values for R^2adj in all models. Response surfaces for *T* and K_p are shown in **Fig. 3**.

Table 3 – Full quadratic models for each response (Coded units)

Term	T	K_p	$\sigma^2 K_p$	$\sigma^2 T$	$FA_{1\ \mu(T)}$	$FA_{2\ \sigma^2(Kp)}$	$FA_{3\ \sigma^2(T)}$	$FA_{4\ \mu(Kp)}$
Constant	7.925	10.622	0.514	0.852	0.659	-0.398	-1.015	-0.348
V	-1.251	-0.238	0.927	0.998	0.533	0.299	0.514	0.459
f	-2.341	-2.584	1.007	1.001	0.505	0.274	0.232	-0.485
d	-1.639	-2.861	0.859	0.999	0.156	0.203	0.231	-0.725
V^2	0.265	-0.196	0.430	0.893	-0.162	0.083	0.520	0.055
f^2	1.577	0.297	0.357	1.312	-0.631	0.011	0.874	0.092
d^2	0.452	0.822	0.655	0.073	-0.111	0.445	-0.027	0.305
$V*f$	0.750	-0.165	0.834	0.104	-0.437	0.559	-0.172	-0.222
$V*d$	0.075	0.217	1.564	0.149	-0.136	0.994	-0.262	0.128
$f*d$	0.675	0.545	0.680	0.247	-0.261	0.429	0.059	0.168
R^2adj. (%)	83.99	96.76	89.61	100.00	97.71	100.00	99.48	87.74

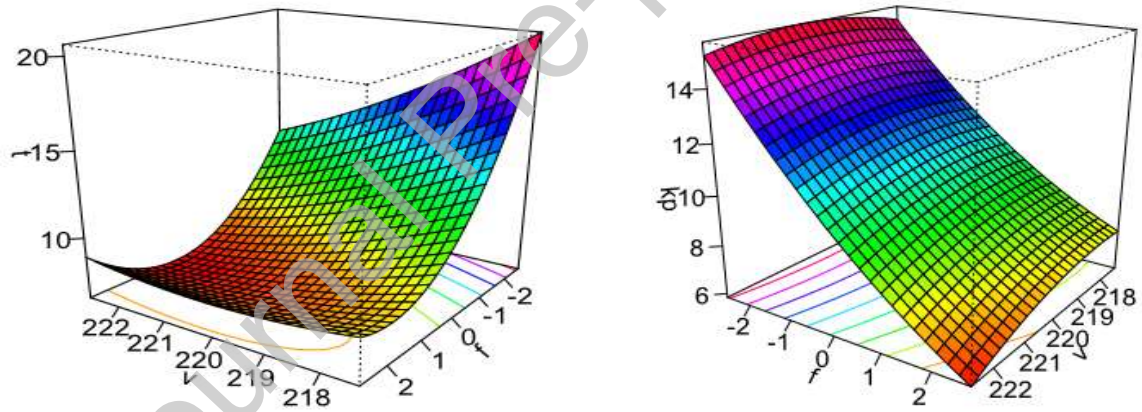

(a) (b)

Fig. 3 - RSM for T (a) and K_p (b).

According to **Step 2**, FA is performed for T, K_p, $\sigma^2(T)$ and $\sigma^2(Kp)$. Extracting four factors using principal component analysis and Equimax rotation it is obtained the following PCFA analysis (**Table 4**). The percent of variability explained by the common factors (or communality) is the same for each one of the four factors and equals to 1. The respective four factor scores are listed in **Table 5**.

Table 4 – Sorted Rotated Factor Loadings.

Variable	Loadings			
	FA_1	**FA_2**	**FA_3**	**FA_4**
$\mu(T)$	**-0.899**	-0.182	-0.133	0.375
$\mu(K_p)$	-0.435	-0.187	-0.303	**0.827**
σ^2 (T)	0.137	0.362	**0.880**	-0.277
σ^2 (K_p)	0.178	**0.909**	0.336	-0.172
Variance	1.0482	1.0246	0.9965	0.9306
% Var	0.262	0.256	0.249	0.233

Table 5 – CCD for Equimax Rotated Factor Scores of the original responses.

Runs	Block	*V*	*f*	*d*	FA_1	FA_2	FA_3	FA_4
1	1	200.00	0.0500	0.1500	-2.1907	1.3354	-1.0133	0.9159
2	1	240.00	0.0500	0.1500	0.4261	-1.2244	0.9260	2.3144
3	1	200.00	0.1000	0.1500	-0.0684	-0.0737	-0.3431	-0.1157
4	1	240.00	0.1000	0.1500	0.3823	-0.3488	0.8766	0.1529
5	1	200.00	0.0500	0.3000	-0.7881	-1.1208	-0.1046	-0.9087
6	1	240.00	0.0500	0.3000	0.8830	0.3442	0.7609	0.7856
7	1	200.00	0.1000	0.3000	-0.1037	-0.7679	0.7705	-1.4992
8	1	240.00	0.1000	0.3000	0.2240	2.8871	0.9738	-0.4681
9	1	220.00	0.0750	0.2250	0.2635	-0.3681	-1.0948	-0.7565
10	1	220.00	0.0750	0.2250	1.3110	-0.4480	-0.8906	0.3077
11	2	187.34	0.0750	0.2250	-0.2140	-0.6963	-0.4002	-0.5819
12	2	252.66	0.0750	0.2250	0.5054	0.3662	1.1498	0.1525
13	2	220.00	0.0342	0.2250	-2.6098	-0.7255	0.8671	0.1919
14	2	220.00	0.1158	0.2250	0.3705	0.0134	1.7713	-0.4508
15	2	220.00	0.0750	0.1025	0.0817	0.4695	-1.3986	1.9008
16	2	220.00	0.0750	0.3475	0.4694	1.1332	-0.7681	-0.9792
17	2	220.00	0.0750	0.2250	1.0687	-0.4308	-0.9421	0.0461
18	2	220.00	0.0750	0.2250	-0.0107	-0.3448	-1.1405	-1.0076

The loadings are weighted eigenvectors and represent the correlation between an original variable and a factor: hence, the greater the loading (in absolute values), the greater the correlation. Therefore, it is possible to verify that FA_1 is the better representative of $\mu(T)$ with a negative correlation. This means that desiring the maximization of $\mu(T)$, FA_1 must be minimized. Such individual minimization leads to the target value for FA_1. Analogously, the minimization of $\mu(K_p)$ will be achieved when FA_4 is minimized (positive correlations/loadings); the minimization of FA_3 and FA_2 will lead to minimization of σ^2 (T) and σ^2 (K_p), respectively. This is the common logic used when original objective functions are replaced by factor scores.

When writing the MSE-FA index for the tool life, for example, we observe that both $(FA_1 - T_{FA1})^2$ and FA_3 must be minimized which implies that MSE-FA may also be minimized. This will represent the minimization of both $[\mu(T) - \text{Target}(T)]^2$ and σ^2 (T) in a multivariate perspective. The same behavior can be verified with the factors associated to Kp. Then, the use of sums as an agglutination operator is a suitable choice to compose MSE-FA index in this case.

Following the procedure established in the **Step 3**, the targets for the MSE's functions are calculated using the GRG algorithm with $\mathbf{x}^T\mathbf{x} \leq \rho^2$ as a unique constraint. This constraint represents the spherical region of a CCD with axial distance (ρ) equals to 1.633 for a design with k = 3 control factors (and 2 blocks). This procedure results in targets for FA_1 and FA_4 respectively equal to $T_{FA_{(\mu)1}}$ = -2.096 and $T_{FA_{(\mu)4}}$ = -1.407.

Table 6 – Payoff matrix of MSE´s, original objective functions and rotated factor scores.

	Min	Min	Min	Min	Max	Min	Min	Min	Min	Min
	MSE_1 (T)	**MSE_2** (Kp)	μ (Kp)	σ^2 (Kp)	μ (T)	σ^2 (T)	FA_4 μ(Kp)	FA_2 σ^2 (Kp)	FA_3 σ^2 (T)	FA_1 μ(T)
MSE_1	**-1.292**	6.971	17.417	2.132	15.262	0.039	0.969	1.323	-1.420	-1.607
MSE_2	5.004	**-1.290**	7.615	0.000	7.832	3.105	-1.305	-1.300	0.414	0.177
μ (K_p)	4.557	1.946	**6.328**	5.880	7.391	6.528	-0.912	1.700	1.326	-0.168
σ^2 (K_p)	2.480	1.362	12.720	**0.000**	10.460	0.314	-0.061	-0.450	-1.099	-0.074
μ (T)	0.203	5.496	17.440	0.813	**17.505**	1.605	0.893	0.203	0.031	-2.380
σ^2 (T)	0.863	2.748	14.292	0.381	11.921	**0.000**	0.259	-0.029	-1.284	-0.500
FA_4	4.552	-1.139	7.669	0.000	7.789	2.401	**-1.407**	-1.140	-0.092	0.190
FA_2	7.222	7.239	14.221	0.000	10.361	3.309	1.460	**-1.150**	1.305	0.467
FA_3	-1.171	7.111	17.466	2.138	15.204	0.000	0.996	1.334	**-1.444**	-1.573

FA_1	-0.547	7.835	18.433	1.338	17.086	0.813	1.259	0.725	-0.564	**-2.096**

Values in bold indicate the optimal result for individual optimization of respective function.

Continuing the procedure, in the **Step 4**, **MSE(FA)$_1$** (referring to T) and **MSE(FA)$_2$** (referring to K_p) are considered. Their individual optimization leads to the anchor points (utopia and nadir) for **MSE(FA)$_1$** equals to [-1.292, 5.004] and [6.971, -1.290] for **MSE(FA)$_2$**. These values are used to generate the scaled functions that composes the NBI-FA. All the individual optima are listed in **Table 7**.

In order to complete the procedure of **Step 4**, the multi-objective non-linear optimization algorithm of Eq. (20) is iteratively performed using GRG for different weights, forming the Pareto frontier for **MSE(FA)$_1$** and **MSE(FA)$_2$** (relative to Kp) depictured in **Fig. 4**. Simultaneously, while NBI-FA method is running for **MSE(FA)$_1$** and **MSE(FA)$_2$**, the value of several others full quadratic models under analysis may be observed and stored. A summary of these metrics is shown in **Table 7** and **Table 8**.

Table 7 - Results of Pareto frontier for **MSE(FA)$_1$ (T)** and **MSE(FA)$_2$ (K_p).**

w_1	**MSE_1 (T)**	**MSE_2 (K_p)**	V	f	d	$\mu(K_p)$	$\sigma^2(K_p)$	$\mu(T)$	$\sigma^2(T)$
0.00	4.47	-0.96	-1.50	0.64	0.08	8.94	0.0000000	8.72	2.5157
0.05	3.92	-0.87	-1.55	0.51	0.05	9.26	0.0000000	9.05	2.2697
0.10	3.35	-0.79	-1.59	0.38	0.04	9.53	0.0000004	9.40	2.0644
0.15	2.77	-0.73	-1.61	0.25	0.05	9.79	0.0000003	9.78	1.8921
0.20	2.19	-0.68	-1.63	0.10	0.07	10.03	0.0000000	10.20	1.7478
0.25	1.60	-0.63	-1.63	-0.05	0.10	10.30	0.0000000	10.69	1.6288
0.30	1.02	-0.58	-1.61	-0.23	0.13	10.60	0.0000000	11.27	1.5358
0.35	0.45	-0.51	-1.56	-0.44	0.18	11.00	0.0000001	12.01	1.4768
0.40	-0.07	-0.39	-1.44	-0.74	0.23	11.66	0.0000000	13.15	1.4931
0.45	-0.32	0.06	-1.38	-0.86	0.10	12.47	0.2664575	14.01	1.4728
0.50	-0.48	0.60	-1.42	-0.81	-0.10	13.02	0.6306150	14.24	1.3382
0.55	-0.62	1.18	-1.42	-0.77	-0.26	13.55	0.9461661	14.41	1.1987
0.60	-0.73	1.77	-1.40	-0.75	-0.40	14.05	1.2144747	14.56	1.0589
0.65	-0.84	2.38	-1.36	-0.73	-0.52	14.54	1.4408286	14.70	0.9210
0.70	-0.93	3.00	-1.32	-0.72	-0.63	15.01	1.6298717	14.84	0.7862
0.75	-1.01	3.64	-1.28	-0.71	-0.73	15.46	1.7850604	14.96	0.6554
0.80	-1.08	4.30	-1.22	-0.71	-0.82	15.90	1.9086717	15.08	0.5294
0.85	-1.13	4.96	-1.16	-0.72	-0.90	16.33	2.0018928	15.20	0.4090
0.90	-1.17	5.65	-1.09	-0.72	-0.98	16.75	2.0648158	15.31	0.2949
0.95	-1.19	6.36	-1.01	-0.74	-1.05	17.16	2.0962596	15.41	0.1883
1.00	-1.19	7.09	-0.93	-0.75	-1.12	17.57	2.0933746	15.51	0.0903

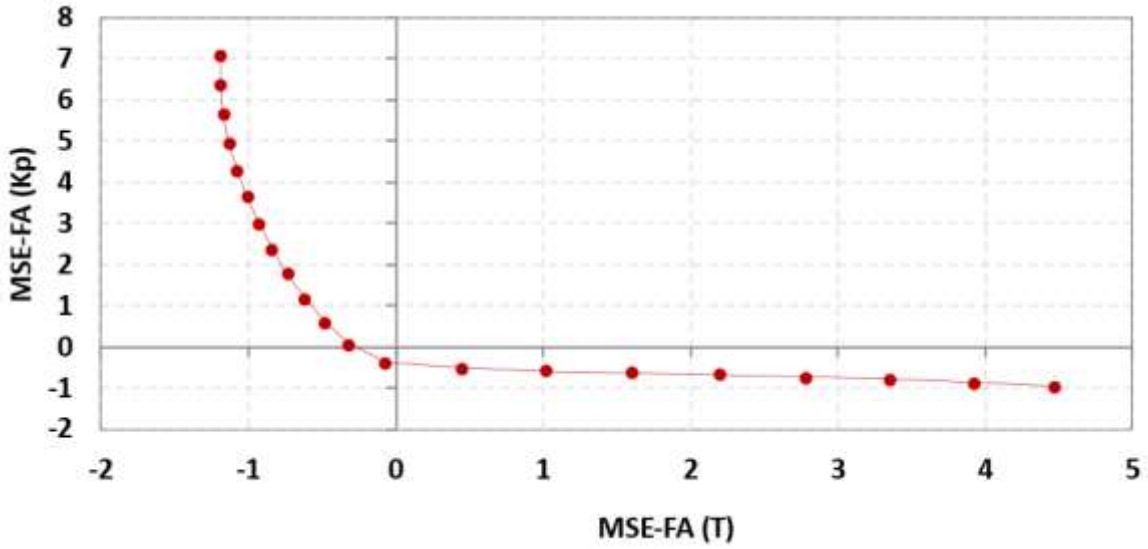

Fig. 4 - Pareto frontier of **$MSE(FA)_1(T)$** and **$MSE(FA)_2(K_P)$**.

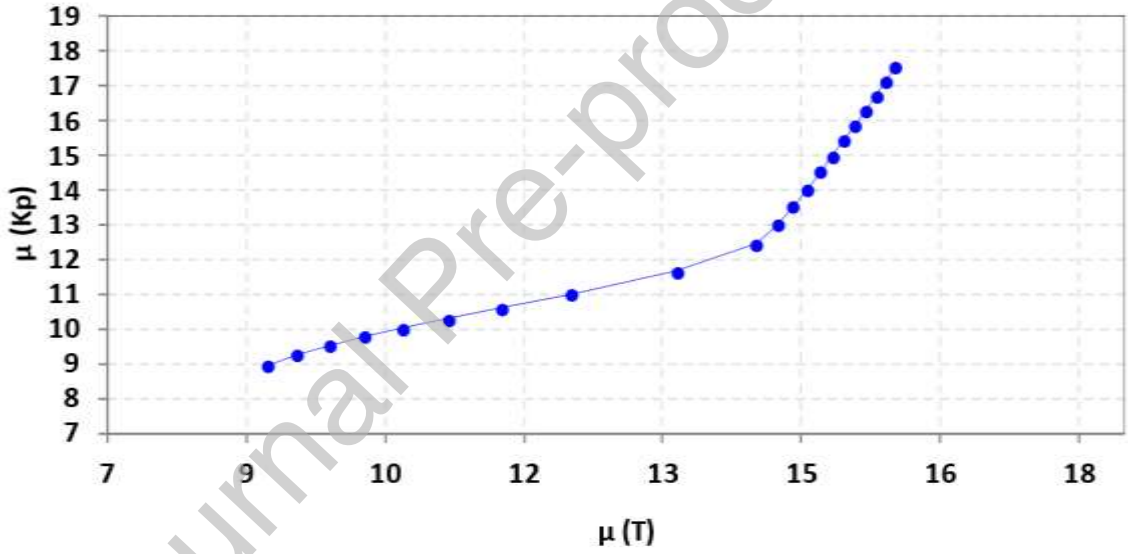

Fig. 5 - Observed values of μ(T) and μ(K_p) from the NBI (MSE-FA) Pareto frontier.

Table 8 presents the results relative to the procedure established at the **Step 5**. Firstly, the Mahalanobis distance between the frontier vectors and their individual targets are calculated. The targets used were μ(T) for T* = 17.505 and μ(K_p) for K_p* = 6.328; MD was determined using the variance-covariance matrix **S** of each solution.

Secondly, 95% confidence ellipses are formed for each Pareto solution and are plotted considering the mean vector as their respective centroids (**Fig. 6)**. Note in this part that all ellipses are based on the $\mathbf{n\hat{\Sigma}}$ variance-covariance matrix, consequently their eigenvalues and eigenvectors are repeated. The center of each ellipse are the pairs resulting from the *μ(T)* and *μ(K_p)* frontier.

Table 8 - Results of Pareto frontier for **MSE(FA)$_1$ (T)** and **MSE(FA)$_2$ (K_p)**.

w_1	FA_4 $\mu(K_p)$	FA_2 $(\sigma^2(K_p))$	FA_3 $(\sigma^2(T))$	FA_1 $(\mu(T))$	MD	V	μ_M	μ_V	Fuzzy (μ^T)
0.00	-1.04	-1.10	0.11	-0.01	10,419.5	0.00248	0.9083	1.00	0.922
0.05	-1.02	-1.02	-0.04	-0.10	21,983.4	0.00125	0.8064	1.00	0.835
0.10	-1.01	-0.95	-0.17	-0.22	8,565.2	0.00336	0.9246	1.00	0.936
0.15	-1.02	-0.89	-0.28	-0.35	9,851.8	0.00301	0.9133	1.00	0.926
0.20	-1.03	-0.83	-0.37	-0.50	17,823.6	0.00171	0.8431	1.00	0.867
0.25	-1.03	-0.77	-0.43	-0.67	91,566.6	0.00034	0.1932	1.00	0.314
0.30	-1.04	-0.72	-0.48	-0.87	31,607.5	0.00104	0.7216	1.00	0.763
0.35	-1.02	-0.66	-0.49	-1.13	22,688.6	0.00156	0.8002	1.00	0.830
0.40	-0.95	-0.60	-0.43	-1.50	113,488.3	0.00036	0.0000	1.00	0.150
0.45	-0.76	-0.36	-0.43	-1.76	22.6	2.46341	0.9999	0.46	0.918
0.50	-0.58	-0.07	-0.57	-1.80	17.1	3.61246	1.0000	0.20	0.880
0.55	-0.41	0.18	-0.70	-1.81	15.5	4.18781	1.0000	0.08	0.861
0.60	-0.24	0.40	-0.81	-1.82	14.9	4.45941	1.0000	0.02	0.852
0.65	-0.07	0.60	-0.92	-1.82	14.7	4.52992	1.0000	0.00	0.850
0.70	0.09	0.77	-1.01	-1.81	14.8	4.45143	1.0000	0.02	0.853
0.75	0.25	0.91	-1.10	-1.80	15.0	4.25345	1.0000	0.06	0.859
0.80	0.40	1.03	-1.18	-1.78	15.4	3.95292	1.0000	0.13	0.869
0.85	0.55	1.13	-1.24	-1.76	16.1	3.55805	1.0000	0.21	0.882
0.90	0.70	1.21	-1.29	-1.74	17.0	3.06848	1.0000	0.32	0.898
0.95	0.85	1.27	-1.33	-1.72	18.4	2.47030	1.0000	0.45	0.918
1.00	1.00	1.30	-1.36	-1.68	21.5	1.70931	0.9999	0.62	0.943

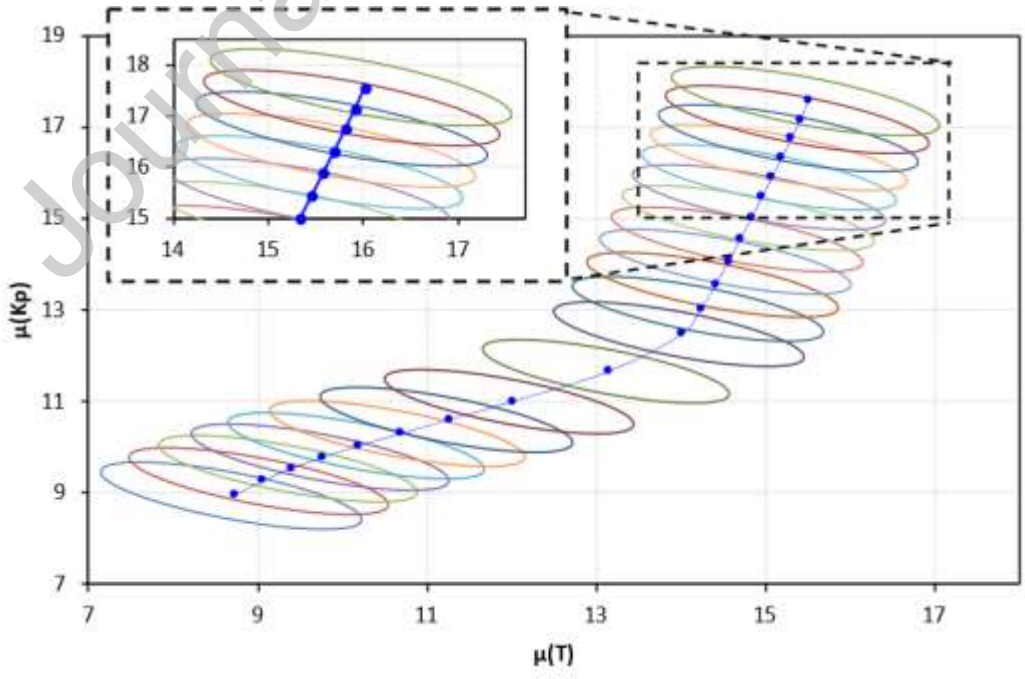

Fig. 6 - Confidence Ellipse for Pareto frontier of **MSE$_1$(T)** and **MSE$_2$(K_P)**.

Complementing the routine of **Step 5**, the volume of each ellipse is calculated using p = 2 and n = 7. In order to obtain 95% confidence ellipses (α=0.05), Eq. (26) is applied to two responses (T and K_p) m = 2, which has a CCD design with 18 observations (n) and response models have 9 coefficients each (r), except for the constant term, as in Eq. (26).

$$\begin{bmatrix} \mathbf{z}_i^{\mathrm{T}}\hat{\boldsymbol{\beta}}(\mathrm{T})_{\mathrm{MWLS}} \\ \mathbf{z}_i^{\mathrm{T}}\hat{\boldsymbol{\beta}}(\mathrm{K_p})_{\mathrm{MWLS}} \end{bmatrix} + \sqrt{\frac{2}{18-9-2}F_{2,5}(0.05)\left[\mathbf{z}^{\mathrm{T}}(\mathbf{x}_i)\left(\mathbf{X}^{\mathrm{T}}\mathbf{W}\mathbf{X}\right)^{-1}\mathbf{z}(\mathbf{x}_i)\right]} \times \begin{bmatrix} 14.236 & 0 \\ 0 & 1.264 \end{bmatrix} \times \begin{bmatrix} 0.937 & 0.351 \\ -0.351 & 0.937 \end{bmatrix} \times \begin{bmatrix} \cos\phi \\ \sin\phi \end{bmatrix} \quad (26)$$

$$\mathbf{n}\hat{\boldsymbol{\Sigma}} = \begin{bmatrix} \left(\mathbf{res}_{\mathrm{T}}\right)^{\mathrm{T}}\mathbf{res}_{\mathrm{T}} & \left(\mathbf{Cov}_{\mathbf{res}_{\mathrm{T}}\times\mathbf{res}_{\mathrm{K_p}}}\right)^{\mathrm{T}}\mathbf{Cov}_{\mathbf{res}_{\mathrm{T}}\times\mathbf{res}_{\mathrm{K_p}}} \\ \left(\mathbf{Cov}_{\mathbf{res}_{\mathrm{T}}\times\mathbf{res}_{\mathrm{K_p}}}\right)^{\mathrm{T}}\mathbf{Cov}_{\mathbf{res}_{\mathrm{T}}\times\mathbf{res}_{\mathrm{K_p}}} & \left(\mathbf{res}_{\mathrm{K_p}}\right)^{\mathrm{T}}\mathbf{res}_{\mathrm{K_p}} \end{bmatrix} = \begin{bmatrix} 12.634 & -4.268 \\ -4.268 & 2.866 \end{bmatrix} \quad (27)$$

Note that the eigenvalues and eigenvectors used are derived from variance-covariance matrix $\mathbf{n}\hat{\boldsymbol{\Sigma}}$, which consists of the relationship between regression residuals of T and K_p). The variance and covariance associated with each point are represented by the ellipse formed, which expresses the uncertainty of that solution found.

In **Step 6**, the membership functions for MD and confidence ellipses volume are calculated. The corresponding values of utopia (1) and nadir (0) are respectively: 14.7 and 113,488.3 for μ_M, 0.00034 and 4.530 for μ_V. Subsequently, with weight of 85/15 between the membership functions, the best value for the Fuzzy decision maker is 0.943 (higher).

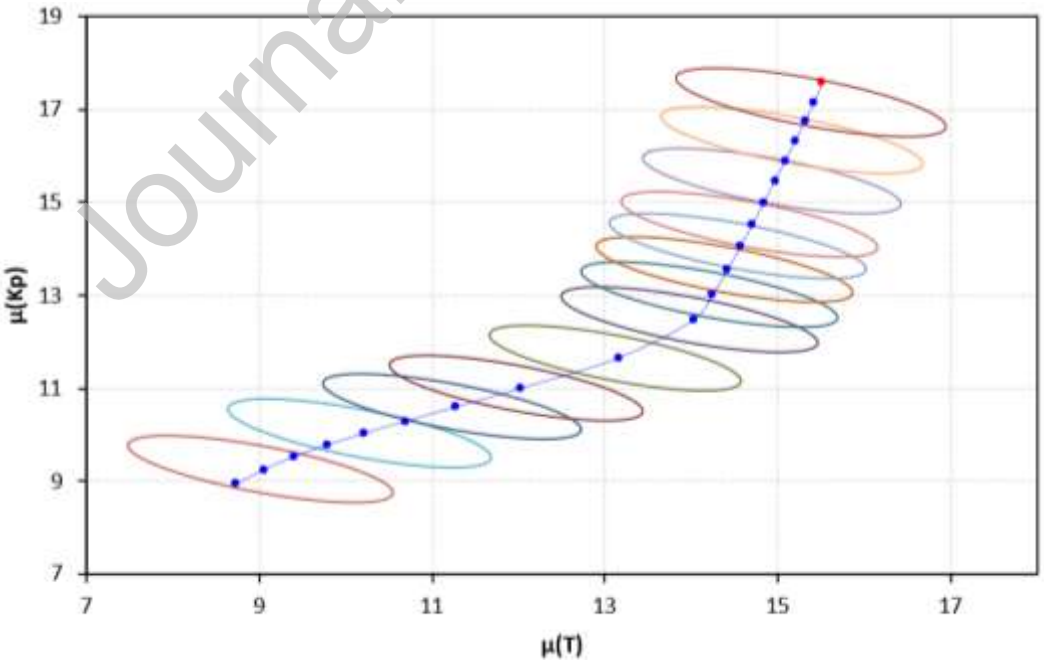

Fig. 7 - Non-Overlapping Confidence Ellipses in Pareto frontier

Therefore, this solution found is point 21 (w=1.0), with cutting speed (V) = 220.4 m/min, Feed rate (f) =0.209 mm/rev and Depth of cut (d) = 0,340 mm. This configuration will promote an expect tool life $\mu(T)$ = 15.51 min and a process cost about $\mu(K_p)$ = 17.57 US$/piece.

Finally, after removing the overlapping ellipses, it is obtained the filtered Pareto frontier shown in the **Fig. 7**. Therefore, this procedure reduces from 21 to 13, the number of optimal scenarios in practice.

The results achieved were better than those achieved by [4], which were: Multivariate optimization K_p = 7.284 US$/piece and T = 5.637 min; Multiple Optimization K_p = 7.410 US$/piece and T = 6.000 min. In both cases, the solution found has a worse relationship between the cost per part (K_p) and the tool life (T).

5.2. Multiobjective optimization of AISI H13 hardened steel turning.

In a similar process of manufacturing hardened steel turning, the same variables are modeled to demonstrate the viability of the proposed method. Although the CCD has the same three input variables (V, f, d), only 2 of the 8 process output responses, tool life (T) and total cost (K_p) are selected for this example. Further information about process data can be found in [5].

The CCD characteristics are: 3 factors, 1 replicate, 19 runs, being 8 cube points, 5 center points in cube, 6 axial points, 0 center points in axial and the distance of each axial point α = 1.68179. **Table 9** represents the DOE of this second case.

The correlation measured between variables T and K_p presents a Pearson coefficient equal to 0.758 (p-value = 0.000). Therefore, it is statistically significant, which is justified for the continuation of **Step 2**.Also analogous to the first numerical example, PCFA is performed for T, K_p, $\sigma^2(T)$ and $\sigma^2(K_p)$, extracting four factors using principal component and Equimax rotation (**Table 10**).

From **Table 10** it is possible to verify that FA_4 replaces μ(T) and presents a negative correlation with this variable; therefore, the minimization of FA_4 leads to the maximization of tool life; FA_3 is positively correlated with σ^2 (T), then its minimization reduces the variance of tool life. FA_1 and FA_2 are positively correlated with $\mu(K_p)$ and σ^2 (K_p), respectively; both minimization reduces the process costs and its respective variances.

Table 9 - Cutting parameters and responses for the CCD 2nd case

Runs	*V*	*f*	*d*	*T*	K_p	$\sigma^2(T)$	$\sigma^2(K_p)$
1	100.00	0.100	0.150	59.50	2.99	33.4	1.008
2	225.00	0.100	0.150	35.50	1.87	4.7	1.012
3	100.00	0.225	0.150	50.50	2.60	1.4	1.003
4	225.00	0.225	0.150	31.00	1.65	16157.5	1.022
5	100.00	0.100	0.330	60.00	3.97	2535.5	1.034
6	225.00	0.100	0.330	29.50	2.31	1.5	1.001
7	100.00	0.225	0.330	50.50	3.33	5.5	1.008
8	225.00	0.225	0.330	29.50	1.41	317.3	1.001
9	57.39	0.163	0.240	59.00	4.20	309.2	1.018
10	267.61	0.163	0.240	28.00	1.48	2970.2	1.005
11	162.50	0.057	0.240	38.00	3.44	27101.7	1.044
12	162.50	0.268	0.240	40.00	1.94	578672.3	1.020
13	162.50	0.163	0.089	49.25	1.81	1.1	1.001
14	162.50	0.163	0.391	48.00	2.56	1.1	1.000
15	162.50	0.163	0.240	44.50	2.57	1.3	1.001
16	162.50	0.163	0.240	44.00	2.54	1.3	1.001
17	162.50	0.163	0.240	45.00	2.61	1.3	1.001
18	162.50	0.163	0.240	45.50	2.53	1.3	1.001
19	162.50	0.163	0.240	44.50	2.50	1.3	1.001

Source: Adapted from Campos [27]

Table 10 - Sorted Rotated Factor Loadings for 2nd case.

	Loadings			
Variable	FA_1	FA_2	FA_3	FA_4
μ(T)	0.433	-0.121	-0.125	**-0.884**
$\mu(K_p)$	**0.915**	-0.034	-0.031	-0.400
σ^2 (T)	-0.039	0.652	**0.744**	0.140
σ^2 (K_p)	-0.053	**0.756**	0.640	0.125
Variance	1.0302	1.0129	0.9798	0.9771
% Var	0.258	0.253	0.245	0.244

Table 11 - Full quadratic models for each response 2nd case

Term	T	K_p	$\sigma^2 K_p$	$\sigma^2 T$	$FA_{1\ \mu(Kp)}$	$FA_{2\ \sigma^2(Kp)}$	$FA_{3\ \sigma^2(T)}$	$FA_{4\ \mu(T)}$
Constant	44.720	2.552	0.001	0.239	0.030	-1.204	-0.524	0.141
V	-10.774	-0.749	0.674	1.104	-0.604	-0.046	0.130	0.948
f	-1.438	-0.342	0.793	1.081	-0.515	0.191	0.123	-0.125
d	-0.666	0.232	0.669	1.073	0.433	0.096	0.187	0.235
V^2	-0.509	0.090	2.004	3.261	0.144	0.151	0.761	0.008
f^2	-2.100	0.037	3.004	3.951	0.169	1.048	0.137	0.151
d^2	1.303	-0.141	0.757	0.725	-0.344	0.476	-0.170	-0.354
*V*f*	1.750	-0.011	1.538	2.804	-0.173	-0.170	0.975	-0.387
*V*d*	-1.000	-0.189	0.365	0.594	-0.278	-0.002	0.157	-0.046
*f*d*	0.500	-0.116	0.914	1.210	-0.234	0.290	0.106	-0.235
R^2 *(adj.)*	92.42	96.74	99.87	99.90	94.22	100.00	99.39	95.55

Table 11 shows the full quadratic models for original responses and respective equimax rotated factor scores. All models present suitable values for R^2 adj. Proceeding to **Step 3**, GRG algorithm are used for calculate the targets for the MSE's functions, nonlinear constraint $\mathbf{x}^T\mathbf{x} \leq 2.828$ (CCD axial distance (ρ) = 1.68179 for k = 3). The result found is **MSE_1 (T)** in $T_{FA_{(\mu)4}}$ = -1.964 and to **MSE_2 (K_p)** in $T_{FA_{(\mu)1}}$ = -1.689.

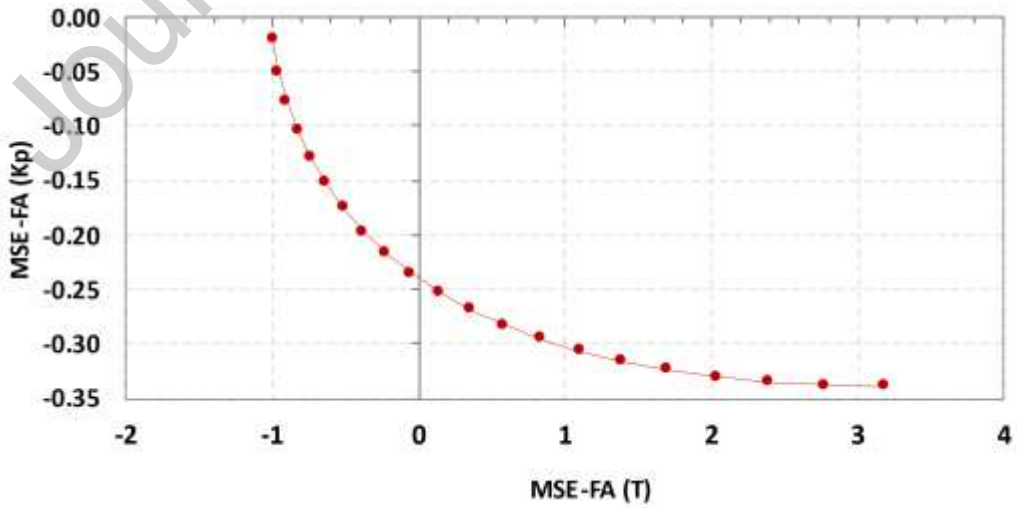

Fig. 8 - Pareto frontier of **MSE_1(T)** and **MSE_2(K_P)** – NBI (MSE-FA) 2nd case

In the **Step 4**, the anchor points are defined as $\mathbf{MSE_1\ (T)}$ = [-0.997, 3.175] and $\mathbf{MSE_2\ (K_p)}$ = [-0.020, -0.339]. NBI method (using GRG) is applied to solve MOP in the MSE of rotated factor scores, forming the Pareto frontier for $\mathbf{MSE_1(}\boldsymbol{T}\mathbf{)}$ and $\mathbf{MSE_2(}\boldsymbol{K_p}\mathbf{)}$, as in **Fig. 8**. The sequence of mean vectors obtained during the optimization of NBI-RFMSE is plotted in **Fig. 9**.

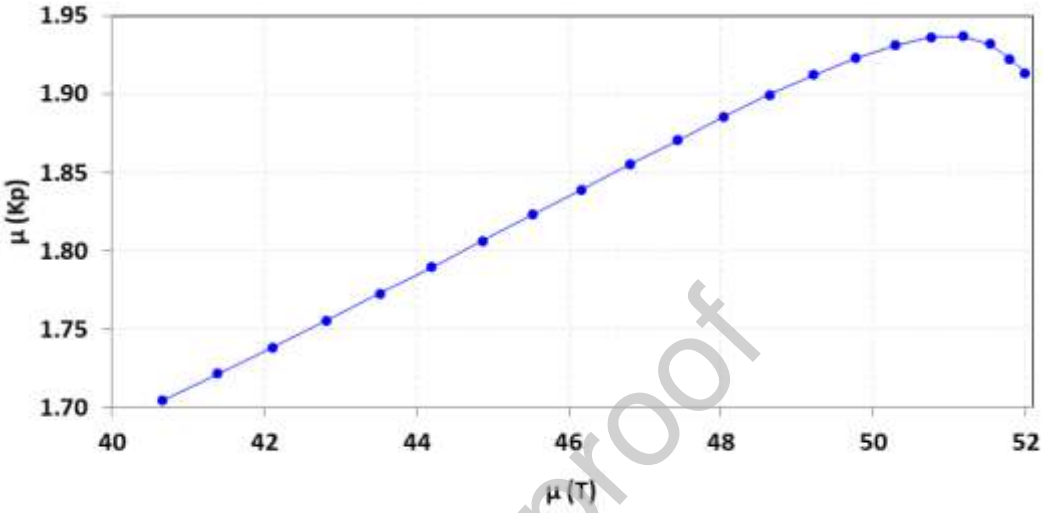

Fig. 9 - Observed values of μ(T) and μ(K_p) from the NBI (MSE-FA) Pareto frontier 2nd case.

After plotting all the confidence ellipses (**Fig. 10**), it is possible to analyze and remove those Pareto points that are overlapping. Of 21 solutions, only 9 remain, as seen in **Fig. 11**. Then, the confidence ellipses volume and MD are calculated with p = 2 and n = 9, using each matrix **S**.

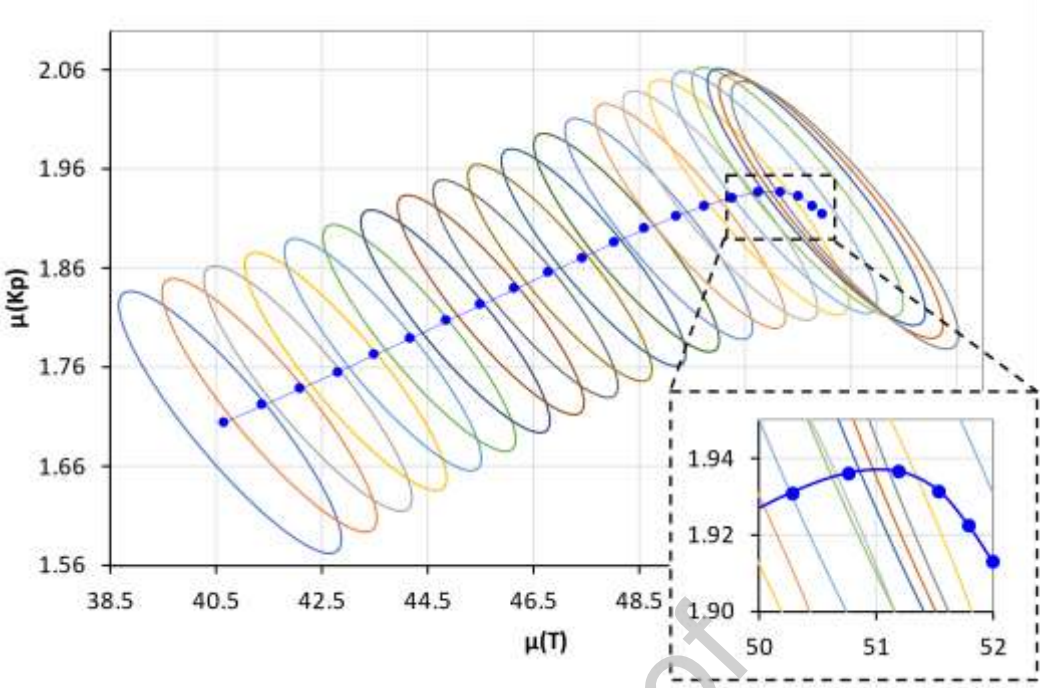

Fig. 10- Confidence Ellipse for Pareto frontier of $\mathbf{MSE_1(T)}$ and $\mathbf{MSE_2(K_P)}$ 2nd case

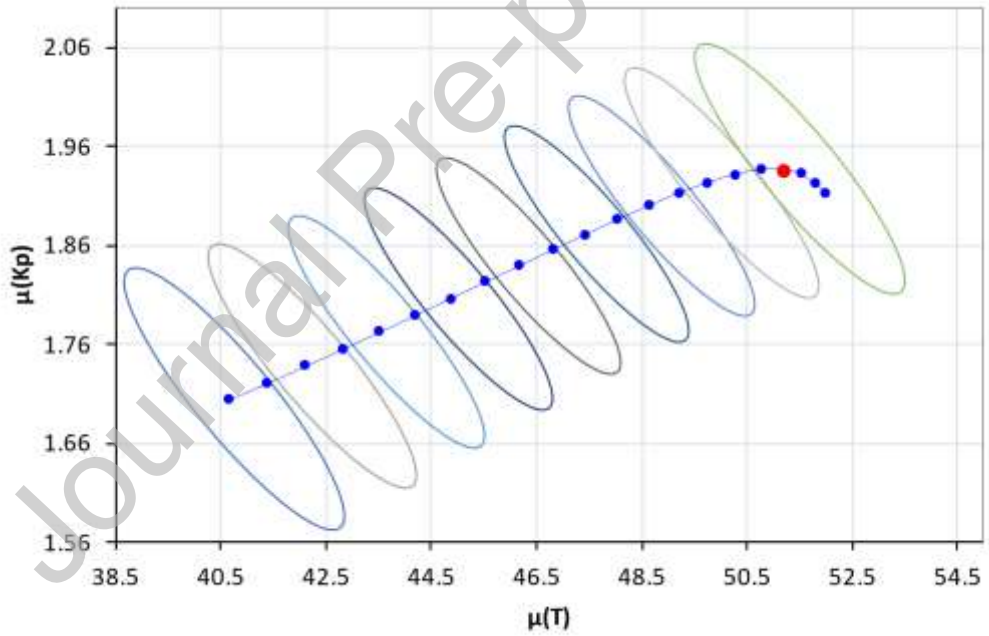

Fig. 11 - Non-overlapping Confidence Ellipses in Pareto frontier 2nd case

Fuzzy decision maker is calculated producing membership functions for MD and V respectively equals to 19.95 and 50.07 for μ_M, 0.87 and 4.83 for μ_V. Given these data, the best overall performance found by decision maker Fuzzy is μ^T = 0.811, relative to the optimum solution point 18 ($w_{1=}$ 0,85), which corresponds to the process settings of Cutting Speed (V) = 178.9 m/min, Feed (f) =0.157 mm/rev and Depth of cut (d) = 0,383 mm. In this way, the

respective response values are $\mu(T)$ = 51.18 min for the mixed ceramic tool life and $\mu(K_p)$ = 1.94 US$/piece for the process cost.

Table 12 - Comparisons among several multi-objective methods

MOP Method	T	Distance	K_p	Distance
Proposed Method	**51.18**	**11.24**	**1.94**	**0.61**
NBI-MMSE*	50.01	12.41	3.29	1.97
NBI*	37.34	25.08	2.34	1.02
WSUM-MMSE*	49.64	12.78	3.26	1.94
MCG-MMSE*	48.16	14.26	2.63	1.31
AHL-MMSE*	50.48	11.94	3.33	2.01
Target	**62.43**		**1.32**	

As a matter of comparison, the multiobjective optimization of this second case study was repeated with several different algorithms available: (a) the NBI-MMSE method like described in Eq. (7), (b) the traditional NBI in four dimensions (NBI*), (c) the method of weighted sums with MMSE functions (WSUM-MMSE*), (d) the Global criterion method (MCG-MMSE*) and the Arc homotopic length (AHL-MMSE*), both with multivariate mean square error function of Eq. (7). These results are summarized in **Table 12**.

As can be noticed, NBI-RFMSE method outperformed all other strategies in this case which suggests that it may be safety used in the optimization of similar manufacturing process.

5. Conclusions

This paper has presented a multi-objective optimization algorithm that combined the characteristics of the Normal Boundary Intersection method with response surface models of equimax rotated factor scores. This hybrid NBI-RFMSE approach allowed the definition of a MSE function using the uncorrelated functions traced for means and variances for each original response of interest. These new objective functions were then optimized using Normal Boundary Intersection method and generated an equispaced Pareto frontier. For each point of this frontier, were established a 95% confidence ellipse based on its respective variances, covariance and expected value. Solutions with overlapped ellipses were removed from the frontier and afterward, they were assessed in terms of their volume (precision) and

accuracy, using a Fuzzy decision-maker index as a matter of balance the both criteria and the decision maker´s preference.

The use of equimax rotated factor scores have presented some advantages over principal components mainly when compared with NBI-MMSE approach: the first one was the ability to fully separate the objective functions – characteristic that was not be achieve with PCA. From an optimization perspective, such separation allows the influence of the weights to be better transmitted to the objective functions. The second advantage is related to the capacity that the rotation method has to undid the conflict between the sense of optimization of the original variable and the response surface model of the factor scores. Equimax method has also presented the advantage to create decomposed functions with the same degree of explanation of total variance observed in the response data. This feature, that was not observed in PCA scores, allowed the definition of functions with the same degree of importance before the weighting process promoted by the interactions of the NBI algorithm.

The use of 95% confidence ellipses proved to be a suitable approach in filtering the initial Pareto optimal solutions, reducing the number of the alternatives for posterior assessment. As the most innovative proposal of this work, this step brought the concept of statistical independence to the context of optimization, discussions which are so rare in the literature.

Two numerical examples were developed to test the approach. In the case of the multi-objective optimization of the turning process of the AISI 52100 hardened steel carried out with CC6050 mixed ceramic inserts the minimal process cost, the maximal tool life, and minimal variance for both responses were achieved with a cutting speed equal to 220.4 m/min, feed rate equal to 0.209 mm/rev and depth of cut equal to 0,340 mm. This configuration will promote an expect tool life of 15.51 with a variance of 0.09 and a process cost about 17.57 US$/piece, with a variance of 2.09. For AISI H13 hardened steel with CC 670 mixed ceramic tools, similar results were achieved with a cutting speed equal to 178.9 m/min, feed rate equal to 0.157 mm/rev and depth of cut equal to 0.383 mm, setup responsible for a tool life of 51.18 min, with a variance of 0.44 and a process cost around 1.94 US$/piece, with a variance of 0.89. It is worth mentioning that the great difference between T and Kp in the numerical cases is due to differences in the type of inserts and in the cost of the steels used.

The quality of these practical results motivates us to suggest the method may be extended to applications on multi-objective optimization problems of many others manufacturing processes.

Acknowledgement: The authors would like to express their gratitude to National Council for Scientific and Technological Development (CNPq), Coordination for the Improvement of Higher Education Personnel (CAPES), Research Support Foundation of Minas Gerais State (FAPEMIG) and Federal University of Itajubá (UNIFEI) for their support in this research.

References

[1] X. Cao, Z. Li, X. Zhou, Z. Luo, J. Duan, Modeling and optimization of resistance spot welded aluminum to Al-Si coated boron steel using response surface methodology and genetic algorithm, Measurement 171 (2021) 108766. https://doi.org/10.1016/j.measurement.2020.108766

[2] Paiva, A.P., Costa, S.C., Paiva, E.J., Balestrassi, P.P., Ferreira, J.R., Multi-objective optimization of pulsed gas metal arc welding process based on weighted principal component scores, Intl. J. Adv. Manuf. Tech. 50 (2010) 113-125. https://doi.org/10.1007/s00170-009-2504-y

[3] P. Sharma, D. Chakradhar, S. Narendranath, Measurement of WEDM performance characteristics of aero-engine alloy using RSM-based TLBO algorithm, Measurement 179 (2021) 109483. https://doi.org/10.1016/j.measurement.2021.109483

[4] A.P. Paiva, J.R. Ferreira, P.P. Balestrassi, A multivariate hybrid approach applied to AISI 52100 hardened steel turning optimization, J. Mater. Process. Technol. 189 (2007) 26-35. https://doi.org/10.1016/j.jmatprotec.2006.12.047

[5] J.H.D. Gaudêncio, F.A. Almeida, R.C. Sabioni, J.B. Turrioni, A.P. Paiva, P.H.S. Campos, Fuzzy multivariate mean square error in equispaced Pareto frontiers considering manufacturing process optimization problems, Eng. Comp. 35 (2019) 1213–1236, https://doi.org/10.1007/s00366-018-0660-0.

[6] L.G.D. Lopes, T.G. Brito, A.P. Paiva, R.S. Peruchi, P.P. Balestrassi, Robust parameter optimization based on multivariate normal boundary intersection, Comput. Ind. Eng. 93 (2016) 55-66. https://doi.org/10.1016/j.cie.2015.12.023

[7] D.M.D. Costa, T.I. Paula, P.A.P. Silva et al., Normal boundary intersection method based on principal components and Taguchi's signal-to-noise ratio applied to the multiobjective optimization of 12L14 free machining steel turning process, Int. J. Adv. Manuf. Technol. 87 (2016) 825–834. https://doi.org/10.1007/s00170-016-8478-7

[8] J.H.D. Gaudêncio, F.A. Almeida, J.B. Turrioni, R.C. Quinino, P.P. Balestrassi, A.P. Paiva, A multiobjective optimization model for machining quality in the AISI 12L14 steel turning process using fuzzy multivariate mean square error, Precis. Eng. 38(3) (2014) 628-638. https://doi.org/10.1016/j.precisioneng.2019.01.001

[9] T.G. Brito, A.P. Paiva, J.R. Ferreira, J.H.F. Gomes, P.P. Balestrassi, A normal boundary intersection approach to multiresponse robust optimization of the surface roughness in end

milling process with combined arrays, Precis. Eng. 56 (2019) pp. 303-320. https://doi.org/10.1016/j.precisioneng.2014.02.013

[10] D.K.J. Lin, W. Tu, Dual response surface optimization, J. Qual. Technol. 27 (1995) 34-39. https://doi.org/10.1080/00224065.1995.11979556

[11] L.C. Tang, K. Xu, A unified approach for dual response surface optimization. J. Qual. Technol. 34 (2002) 437-447. https://doi.org/10.1080/00224065.2002.11980175

[12] G.L. Boylan, P.L. Goethals, B.R. Cho, Robust parameter design in resource-constrained environments: An investigation of trade-offs between costs and precision within variable processes, Appl. Math. Modell. 37 (2013) 2394-2416. https://doi.org/10.1016/j.measurement.2019.07.072

[13] S. Shin, F. Samanlioglu, B.R. Cho, M.M. Wiecek, Computing trade-offs in robust design: perspectives of the mean squared error, Comput. Ind. Eng. 60 (2011) 248-255. https://doi.org/10.1016/j.cie.2010.11.006

[14] J. Kovach, B.R. Cho, A D-optimal design approach to constrained multiresponse robust design with prioritized mean and variance considerations, Comput. Ind. Eng. 57 (2009) 237-245. https://doi.org/10.1016/j.cie.2008.11.011

[15] O. Köksoy, Multiresponse robust design: Mean square error (MSE) criterion, Appl. Math. Comput. 175(2) (2006) 1716-1729. https://doi.org/10.1016/j.amc.2005.09.016

[16] L.G.D. Lopes, T.G. Brito, A.P. Paiva, R.S. Peruchi, P.P. Balestrassi, Robust parameter optimization based on multivariate normal boundary intersection, Comput. Ind. Eng. 93 (2016) 55-66. https://doi.org/10.1016/j.cie.2015.12.023

[17] R.D. Plante, Process capability: a criterion for optimizing multiple response product and process design, IIE Trans. 33 (2001) 497-509. https://doi.org/10.1023/A:1007694030052

[18] I. Das, J.E. Dennis, Normal boundary intersection: A new method for generating the Pareto surface in nonlinear multicriteria optimization problems, SIAM J. Optim. 8 (1998) 631-657. https://doi.org/10.1137/S1052623496307510

[19] A. Ghane-Kanafe, E. Khorram, A new scalarization method for finding the efficient frontier in non-convex multi-objective problems, Appl. Math. Modell. 39 (2015) 7483-7498. https://doi.org/10.1016/j.apm.2015.03.022

[20] N. Bratchell, Multivariate response surface modeling by principal components analysis. J. Chemom. 3(4) (1989) 579-588. https://doi.org/10.1002/cem.1180030406

[21] F.C. Wu, Optimization of correlated multiple quality characteristics using desirability function, Qual. Eng. 17 (2004) 119-126. https://doi.org/10.1081/QEN-200028725.

[22] A.I. Khuri, M. Conlon, Simultaneous optimization of multiple responses represented by polynomial regression functions. Technometrics. 23 (1981) 363-375. https://doi.org/10.1080/00401706.1981.10487681

[23] Paiva, A.P., Paiva, E.J., Ferreira, J.R. Balestrassi, P.P. Costa, S.C. A multivariate mean square error optimization of AISI 52100 hardened steel turning, The International Journal of Advanced Manufacturing Technology 43 (2009) 631-643. http://dx.doi.org/10.1007/s00170-008-1745-5

[24] F.L. Naves, T.I. de Paula, P.P. Balestrassi, W.L.M. Braga, R.S. Sawhney, A.P. Paiva, Multivariate Normal Boundary Intersection based on rotated factor scores: A multiobjective optimization method for methyl orange treatment, J. Clean. Prod. 143 (2017) 413-439. https://doi.org/10.1016/j.jclepro.2016.12.092

[25] R.A. Johnson, D. Wichern, Applied Multivariate Statistical Analysis, 6th ed. Prentice-Hall, New Jersey, 2007.

[26] R.R. Leite, Normal boundary intersection method for quadratic models of rotated factory scores. Dissertation, Federal University of Itajubá, Brazil, 2019. https://repositorio.unifei.edu.br/jspui/handle/123456789/1903

[27] P.H.S. Campos, Metodologia DEA-OTS: Uma contribuição para a seleção ótima de ferramentas no Torneamento do Aço ABNT H13 Endurecido. PhD Dissertation, (2015). Federal University of Itajubá, Brazil. https://repositorio.unifei.edu.br/jspui/handle/123456789/127

[28] E. Zitzler, L. Thiele, M. Laumanns, C.M. Fonseca, V.G. da Fonseca, Performance assessment of multiobjective optimizers: an analysis and review. IEEE Trans. Evol. Comput. 7(2) (2003) 117-132. https://doi.org/10.1109/TEVC.2003.810758

[29] H.J. Zimmermann, Fuzzy programming and linear programming with several objective functions. Fuzzy Sets Syst. 1 (1978) 45-55. https://doi.org/10.1016/0165-0114(78)90031-3

[30] R.H. Myers, D.C. Montgomery, G.G. Vining, Generalized Linear Models – With applications in Engineering and the Sciences, Wiley, (2002).